International Institute for Applied Systems Analysis
IIASA www.iiasa.ac.at

Influence of four major plant traits on average height, leaf-area cover, net primary productivity, an biomass density in single-species forests: A theoretical investigation

Falster, D.S., Brannstrom, A., Dieckmann, U. and Westoby, M.

IIASA Interim Report
June 2010

International Institute for
Applied Systems Analysis
Schlossplatz 1
A-2361 Laxenburg, Austria

Tel: +43 2236 807 342
Fax: +43 2236 71313
E-mail: publications@iiasa.ac.at
Web: www.iiasa.ac.at

Interim Report **IR-10-036**

Influence of four major plant traits on average height, leaf-area cover, net primary productivity, and biomass density in single-species forests: A theoretical investigation

Daniel S. Falster (daniel.falster@mq.edu.au)
Åke Brännström (ake.brannstrom@math.umu.se)
Ulf Dieckmann (dieckmann@iiasa.ac.at)
Mark Westoby (mark.westoby@mq.edu.au)

Approved by

Detlof Von Winterfeldt
Director

July 2011

TITLE: Influence of four major plant traits on average height, leaf-area cover, net primary productivity, and biomass density in single-species forests: a theoretical investigation

JOURNAL: Journal of Ecology

AUTHORS: Daniel S. Falster[1], Åke Brännström[2,3], Ulf Dieckmann[3], Mark Westoby[1]

1 – Department of Biological Sciences, Macquarie University NSW 2109, Sydney, Australia

2 – Department of Mathematics and Mathematical Statistics, Umeå University, 901-87 Umeå, Sweden

3 – Evolution and Ecology Program, International Institute for Applied Systems Analysis, Schlossplatz 1, 2361, Laxenburg, Austria

CORRESPONDING AUTHOR: Daniel S. Falster, daniel.falster@mq.edu.au, Ph: +612-9850-9258, Fax: +612-9850-8228

RUNNING TITLE: Influence of functional traits on emergent vegetation properties

SUMMARY

1. Numerous plant traits are known to influence aspects of individual performance, including rates of carbon uptake, tissue turnover, mortality and fecundity. These traits are bound to influence emergent properties of vegetation because quantities such as leaf-area cover, average height, primary productivity and density of standing biomass result from the collective behaviour of individuals. Yet, little is known about the influence of individual traits on these emergent properties, despite the widespread use in current vegetation models of plant functional types, each of which is defined by a constellation of traits.
2. We examine the influence of four key traits (leaf economic strategy, height at maturation, wood density, and seed size) on four emergent vegetation properties (average height of leaf

area, leaf-area index, net primary productivity and biomass density). We employ a trait-, size- and patch-structured model (TSPM) of vegetation dynamics that allows scaling up from individual-level growth processes and probabilistic disturbances to landscape-level predictions. A physiological growth model incorporating relevant trade-offs was designed and calibrated based on known empirical patterns. The resulting vegetation model naturally exhibits a range of phenomena commonly observed in vegetation dynamics.

3. We modelled single-species stands, varying each trait over its known empirical range. Seed size had only a small effect on vegetation properties, primarily because our metapopulations were not seed-limited. The remaining traits all had larger effects on vegetation properties, especially on biomass density. Leaf economic strategy influenced minimum light requirement, and thus total leaf area and basal area. Wood density and height at maturation influenced vegetation mainly by modifying individual stem mass. These effects of traits were maintained, and sometimes amplified, across stands differing in productivity and mean disturbance interval.
4. Synthesis: Natural trait variation can cause large differences in emergent properties of vegetation, the magnitudes of which approach those arising through changes to site productivity and disturbance frequency. Our results therefore underscore the need for next-generation vegetation models that incorporate functional traits together with their effects on the patch and size structure of vegetation.

Keywords: allometry, ecosystem services, functional traits, height, leaf-area index, net primary productivity, partial differential equation, size-asymmetric competition, vegetation model, determinants of plant community diversity and structure

Glossary: DGVM =Dynamic global vegetation model, LAI = leaf-area index, LMA = leaf mass per unit area, NPP = net primary productivity, PDE = partial differential equation, TSPM = trait-size-patch-structured vegetation model

INTRODUCTION

Emergent properties of vegetation are those that result from the collective behaviour of individuals, such as average canopy height, leaf-area cover, biomass production rates and biomass density. These quantitative features are of fundamental importance in ecosystems. Autotrophic production and the vertical structure of vegetation provide the foundations for terrestrial biodiversity, in terms of supplying food, adjusting microclimate and creating habitat. Canopies exchange heat and water with the atmosphere, and modulate runoff and soil erosion. Through shifting carbon concentration in the atmosphere, vegetation can also alter global climate over the longer term. In summary, vegetation structure and function can influence processes ranging from the formation and maintenance of complex food webs to regional weather, soil development and regulation of global climate (Shukla & Mintz 1982; Bonan 2008).

Potential influences on emergent vegetation properties include climate, nutrient supply, disturbance regime and the traits of component species. Species traits are perceived as important drivers of vegetation structure, and this is illustrated by the near-universal adoption of the functional-type paradigm in dynamic global vegetation models (DGVMs) (Cramer et al. 2001; Bonan & Levis 2002; Sitch et al. 2008). Plant functional types are archetypal plant species that differ from each other in terms of their trait values. One rationale for incorporating these different types into DGVMs is their influence on emergent vegetation properties. Trait variation is also thought to underpin relationships widely observed in small-scale manipulative experiments between species diversity and various aspects of ecosystem function (Tilman et al. 1997; Hector & Bagchi 2007).

Yet, little is known about the actual influence of individual traits on vegetation properties, despite the implied importance of traits.

There are several reasons why it remains poorly understood how the traits of species influence emergent properties of vegetation. One is that manipulative experiments at the required spatial scale and timeframe are very difficult. While numerous experiments have used short-lived herb and grass species, most of these studies were designed to capture the effects of species diversity on vegetation dynamics, rather than the effects of traits *per se* (reviews by Hooper et al. 2005; Hector & Bagchi 2007). A second reason is that, although most DGVMs notionally include quite a large number of traits, the tradeoffs and correlations between different traits in these models do not yet reflect the big advances that were made in trait research over the past decade. Third, but perhaps most crucially, many contemporary vegetation models lack the internal population structure required for the effects of traits to be properly described and manifested.

Scaling effectively from traits, which control the allocation decisions of individuals, to emergent properties of vegetation requires individual-scale growth processes to be integrated with the population- and community-level demographic processes determining the size distribution of plants across a landscape (Prentice & Leemans 1990; Moorcroft, Hurtt, & Pacala 2001; Purves & Pacala 2008). Since the direct influence of traits is on individual rates of growth, fecundity and mortality, size distributions are needed to integrate these effects over a heterogeneous population. Two of the most important factors influencing the number and size of individuals in a landscape are disturbance and size-asymmetric competition for light (Goff & West 1975; Hara 1984; Shugart 1984; Coomes & Allen 2007). By removing established individuals, disturbances remove standing biomass and increase local light levels, thereby promoting growth and recruitment. Similarly, success within developing stands depends critically on the amount of shading from local competitors. To account for the influences of these processes on size distributions, models would ideally describe a continuous distribution of individual sizes. However, many vegetation models – including all major

DGVMs (reviewed by Cramer et al. 2001; Sitch et al. 2008) – group individuals within each species into a single size class. This limitation renders them unable to capture the full, dynamic effects of competition, disturbance and trait variation on emergent vegetation properties.

There are several ways in which size structure can be introduced when modelling vegetation (Busing & Mailly 2004). Individual-based, spatially explicit, stochastic simulators such as SORTIE (Pacala et al. 1996) offer the greatest level of ecological realism and detail. However, these models are also computationally intensive, which inhibits their widespread application (Levin et al. 1997). Computational speed can be improved by focussing on the vertical structure of local populations within patches of vegetation, while neglecting fine-scale spatial interactions within patches, as well as the spatial configuration among patches. Models taking this approach have been widely applied since the 1970s and shown to capture a wide range of phenomena (e.g. Shugart 1984; Huston & Smith 1987; Huston & DeAngelis 1987; Prentice & Leemans 1990; Bugmann 2001). However, the stochastic nature of gap models makes it difficult to separate the underlying signal of ecological processes from intrinsic random variation. Models formulated using partial differential equations (PDEs) offer a possible solution. By approximating individual-level and patch-level processes with PDEs, the influences of traits, climate, size-structured competition for light and probabilistic disturbance can be analysed in a deterministic fashion (Sinko & Streifer 1967; Levin & Paine 1974; Hara 1984; Metz & Diekmann 1986; Kohyama 1993; Moorcroft, Hurtt, and Pacala 2001). Such PDE-based models are also known as physiologically structured population models (Metz & Diekmann 1986; de Roos 1997) or as size- and age-structured approximations (Moorcroft, Hurtt, and Pacala 2001). These models have already been shown to predict a range of phenomena in line with empirical data, including patterns of growth within developing stands (Hara 1984; Yokozawa & Hara 1992) and stem-diameter distributions (Kohyama 1993), as well as temporal patterns of species dominance, biomass accumulation and net ecosystem production (Moorcroft, Hurtt, and Pacala 2001; Medvigy et al. 2009).

In this study, we consider a metapopulation of patches that are linked through dispersal and are subject to probabilistic patch-level disturbances. The vegetation dynamics in each patch are structured with respect to size, and potentially with respect to traits. We therefore refer to the resultant model as a trait-, size-, and patch-structured model, or TSPM. We use such a TSPM to examine the influence on emergent properties of vegetation of four functional traits: leaf economic strategy, height at maturation, wood density and seed size. These traits have been chosen because they are known to vary widely among species, because the underlying trade-offs are relatively well understood and because they highlight important alternative ways of altering a plant's life history (Westoby et al. 2002; Wright et al. 2004; Chave et al. 2009). We chose four emergent properties that describe some fundamental influences of vegetation on food webs, nutrient cycles and land-surface interactions: average height of leaf area, leaf-area index (LAI), net primary productivity (NPP) and density of standing biomass per ground area (biomass density). Therefore, the goals of this paper are:

1) to derive a trait-size-patch-structured vegetation model;

2) to quantify the modelled influence of four life-history traits on average height of leaf area, LAI, NPP and biomass density; and

3) to assess the sensitivity of trait effects to shifts in site productivity and disturbance frequency.

MATERIALS AND METHODS

We consider a trait-, size- and patch-structured metapopulation of plants subject to probabilistic disturbances and competition for light. As such, the model is most applicable to forests. Each element of the model draws on well-established physiology and ecology. Fig. 1 gives an overview of the main features, described in more detail below. Corresponding equations and parameters are summarised in Table 1 and Table 2. Additional details regarding model derivation, confirmation and parameterisation are given in the Supporting Information.

SIZE- AND PATCH-STRUCTURED METAPOPULATION

We consider a spatially unstructured metapopulation consisting of a large number of patches linked by dispersal (Fig. 1). Each patch is assumed to contain a large number of individuals. All patches are subject to probabilistic disturbances that remove all individuals in a patch. For this analysis, we assume that the risk of disturbance increases linearly with patch age, defined as the time since the last disturbance. Under this assumption, disturbance intervals follow a Weibull probability distribution (Clark 1989), leading to an analytic solution for the equilibrium distribution of patch ages in the metapopulation defined by a single parameter: the mean disturbance interval (eqn 23; see Appendix S1 in Supporting Information). With the same mean disturbance interval, different disturbance regimes cause only small variations in the predicted age distribution (McCarthy, Gill, & Bradstock 2001), indicating that results are not particularly sensitive to the specific function chosen. Seeds produced in all patches contribute to a global seed rain, from which newly disturbed patches are colonised. Seeds continue to arrive over the lifespan of a patch; however, only seedlings able to maintain positive mass production successfully establish (see below).

Competitive hierarchies within developing patches were modelled by tracking the size distribution of plants, as patches age after a disturbance (eqn 22) (Kohyama 1993; de Roos 1997; Moorcroft, Hurtt, and Pacala 2001). This distribution evolves as: 1) seedlings enter the population after germination, 2) growth of established plants moves them up in the size spectrum and 3) mortality removes plants from the population. Growth and mortality rates (eqn 19, 21) vary with an individual's net dry-matter production rate, which in turn is influenced by shading from other plants in the patch. Following Yokozawa and Hara (1995), we let the leaf area of each individual be distributed over its height according to a distribution governed by a single crown-shape parameter (eqn 9-10; see Appendix S2 for details). This vertical leaf-area distribution combines with the distribution of plant sizes in the patch to give cumulative levels of shading down through the canopy (eqn 11). The outcome of this model structure is strong size-asymmetric competition:

168 relatively larger plants continue to grow, while relatively smaller plants are suppressed and removed
169 from the stand.

170 Net dry-matter production is determined by three factors: an individual's size, its traits, and the
171 degree of shading imposed by its competitors (eqn 15). Gross carbon-dioxide (CO_2) assimilation for
172 each individual is calculated by integrating instantaneous photosynthetic rates, at corresponding
173 light levels, over its leaf area (eqn 12). Maintenance respiration, growth respiration and tissue
174 turnover are then accounted for in calculating net dry-matter production. Maintenance respiration
175 increases linearly with the total nitrogen content of leaves, total mass of roots and total volume of
176 sapwood and bark (eqn 13). Bark respiration was set at twice the sapwood respiration, in
177 accordance with observing an average nitrogen content in bark that is approximately twice as high
178 as that of sapwood (Martin et al. 1998). Leaf-turnover rate was set to vary as a function of leaf mass
179 per unit area (LMA), while bark and fine-root turnover were set to a fixed rate (eqn 14). Since total
180 leaf area increases throughout ontogeny, potential gross assimilation also increases. At the same
181 time, an increasing fraction of a plant's mass is occupied in support tissues (stem, bark and
182 heartwood) (eqn 4-8), so the total burden of respiration and tissue turnover also increases with size
183 (Fig. S6). Consequently, as size increases, the relative growth rate decreases and the minimum light
184 level needed to maintain a positive mass production increases (Fig. S6).

185 With increasing size, individuals allocate a greater fraction of newly produced dry matter to
186 reproduction (eqn 16). Height at maturation is one of the considered functional traits; around this
187 size, allocation to reproduction makes a rapid transition from almost 0% to 100%. This allocation
188 pattern closely approximates the bang-bang strategy derived by theoretical investigations (Mäkelä
189 1985; Iwasa 2000). Fecundity rates are calculated directly from mass allocated to reproduction via
190 seed mass. To account for the various accessory costs of seed production, we let each unit of seed
191 mass be accompanied by a fixed mass representing flowers, fruits, and dispersal structures (eqn 16).

Individuals in the model are exposed to three sources of mortality: 1) disturbance-driven mortality, which occurs at the scale of whole patches; 2) intrinsic mortality, which varies among species according to their wood density (eqn 21), and 3) growth-related mortality, which varies among individuals within a patch according to their net mass production per unit leaf area (eqn 21). The equation for intrinsic mortality was motivated by an empirical relationship relating wood density to average mortality (see Appendix S4 for details). An exponential increase in growth-related mortality with declining mass production implies that this mortality heavily affects shaded individuals (King et al. 2006; Coomes & Allen 2007; Baltzer & Thomas 2007), as well as maladapted plants. We let growth-related mortality be determined by production per unit leaf area, rather than by total production, so that mortality did not depend strongly on size as such.

Survival of seedlings through germination was also made a function of production per leaf area (eqn 20). Equation 20 was chosen so that both seedling survival and the density of plants at the smallest size declined to zero as dry mass production declined to zero (see Appendix S5 for details). In addition, growth, fecundity, survival through germination and density of seedlings at smallest size, are all set to zero when an individual's mass production becomes negative (eqn 17, 19, 20, 22).

ALLOMETRIC RELATIONSHIPS FOR PLANT COMPONENTS

Detailed modelling of size distributions (eqn 22) is facilitated when individuals are organised along a single size dimension. However, to calculate light interception, dry-matter production and growth rate, we need to know the size of all plant components, including an individual's height, as well as the mass of its sapwood, heartwood, bark and roots. Therefore, one component of the model was a set of allometric relationships binding these various components to each other (eqn 2-8, see Appendix S2 for derivations). Functionally, crown size (measured in terms of total leaf area) can be thought of as the primary indicator of an individual's size, but in the equations of the model each component is expressed in relation to total leaf mass, since this resulted in simpler equations. For

illustrating results we have used stem height to express the size of individuals, as this seemed easiest for readers to envisage.

Our allometric model is inspired by Yokozawa & Hara (1995). It assumes fixed ratios of leaf area to sapwood area (Shinozaki et al.'s pipe model,1964) and of leaf area to root mass, as well as an allocation profile between leaf area and height (eqn 3). Bark mass (including true bark and phloem) is modelled using an analogue of the pipe model. Heartwood mass is linked to leaf area using an empirical scaling relationship, which amounts to a different approach from many other models that derive heartwood growth from a rate of sapwood turnover. Various traits can be included to produce strategic differences in allocation among species. However, within any species there remains a single ontogenetic pathway along which individuals are transported through growth processes.

The allocation model described by equations 3-8 was verified using the Coweeta biomass dataset (Martin et al. 1998), which includes data on plant dimensions (leaf area, sapwood mass, bark mass, heartwood mass, height) and traits for individuals spanning a range of sizes in 10 different species. Within species, crown size explained an average of 73% of variation in height, 88% of variation in sapwood mass, 83% of variation in bark mass, and 61% of variation in heartwood mass (Appendix S3). Differences in LMA, wood density, leaf area per unit sapwood area and height-leaf area profile explained differences among species in leaf, sapwood, bark and heartwood mass for plants of given leaf area (Appendix S3). Thus, the model seemed to perform well in approximating allocation patterns within and across species.

LEAF-LEVEL ASSIMILATION AND SITE PRODUCTIVITY

For a given canopy openness, gross annual CO_2 assimilation of a leaf was obtained by integrating instantaneous rates, calculated using a standard rectangular hyperbola (Cannell & Thornley 1998), over the diurnal and seasonal patterns of solar variation experienced at a given latitude and longitude (see Appendix S6 for details). We let maximum photosynthetic rates per unit leaf area be

240 determined by leaf nitrogen content and by the photosynthetic nitrogen-use efficiency (ratio of
241 light-saturated CO_2 assimilation rate to leaf nitrogen mass) of the leaves (Wright et al. 2004). These
242 maximum rates were assumed constant for all individuals in a metapopulation, but were adjusted up
243 and down as a proxy for influences of climate (i.e. rainfall, humidity, temperature) or nutrient
244 supply on growth, and thereby on site productivity. Although these influences could be modelled
245 more mechanistically, by including stomatal and hydraulic sub-models (e.g. Moorcroft, Hurtt, and
246 Pacala 2001; Medvigy et al. 2009), this level of physiological detail was deemed unnecessary for
247 the current study.

248 **TRAITS AND TRADE-OFFS**

249 LEAF ECONOMICS: To model variation in leaf economic strategy, we let leaf turnover be
250 inversely related to LMA (eqn 14), while maintaining a constant nitrogen content per unit leaf area.
251 This relationship captures the widely observed coordination between LMA, average leaf lifespan,
252 nitrogen content per unit leaf mass and maximum assimilation rate per unit leaf mass, known as the
253 leaf economics spectrum (Reich, Walters, & Ellsworth 1992; Wright et al. 2004). Species at the
254 fast-return end of the spectrum, characterised by low LMA and high nitrogen content per unit mass,
255 realise greater mass-specific assimilation rates, but suffer from disproportionately high turnover
256 rates and higher leaf respiration.

257 WOOD DENSITY: The effects of wood density were modelled through a trade-off between the
258 efficiency of stem growth (eqn 4-6) and intrinsic mortality rate (eqn 21), with mortality increasing
259 exponentially as wood density decreases. Two presumed costs of cheaper volumetric growth are an
260 increased risk of infection by pathogens or borers in the stem and decreased structural stability
261 (Chave et al. 2009). These costs could lead to increased mortality rates for stems with lower wood
262 density, independent of the degree of shading. Supporting this idea, we found consistent
263 relationships between low wood density and average mortality rate across species from 4 tropical
264 sites (Appendix S4; see also Muller-Landau 2004; King et al. 2006; Chave et al. 2009).

HEIGHT AT MATURATION: Height at maturation describes the size around which an individual's allocation of net dry-matter production gradually switches from growth to reproduction (eqn 16). (In eqn 16, it is the height at which allocation to reproduction reaches 50% of its maximum value.) Height at maturation thereby influences survival until maturation, subsequent reproductive output, length of the reproductive lifespan, and expected lifetime fecundity.

SEED SIZE: The effects of seed size were modelled through a trade-off between fecundity and size at germination (eqn 1, 17). Large seed size was not treated as conferring any advantage during the seed and establishment phases of the life cycle, but did influence an individual's size when it entered a patch, implying an advantage during the subsequent competitive interactions.

OUTLINE OF ANALYSES

We analysed a series of single-species stands under a solar regime corresponding to Sydney, Australia, with a mean disturbance interval of 30 years. The model was calibrated using a variety of sources, including large multi-site databases and detailed site-specific studies. An overview of the parameters used is given in Table 2; for full details of the parameterisation see Appendix S7. We used the escalator boxcar train technique (de Roos 1997), combined with a fourth-order Runge-Kutta ordinary differential equation solver (Press 1995), to model the dynamics of the vegetation's size distribution (eqn 22).

To assess the influence of traits on vegetation, we varied individual traits over a majority of their known empirical range. For each trait combination, we modelled a metapopulation at demographic equilibrium (where a patch's seed rain equals its seed production) and recorded temporal patterns of stand development and of metapopulation averages for each of the four vegetation properties (eqn 24-27). Available data on height at maturation are limited; consequently, we chose a range from 6-24m, with an intermediate height of 12m. For the other three traits, we described the known empirical range from available databases, adopting the median, fifth, and ninety-fifth percentiles for

289 average, low and high parameter settings. Data for LMA were taken from the GLOPNET dataset
290 (Wright et al. 2004) restricted to trees and shrubs. Data for wood density were taken from a global
291 wood database (Zanne et al. 2009). Data for seed size were taken from a published database (Moles
292 et al. 2004), restricted to species that attain more than 5m height. Each trait was varied across its
293 known range, while the remaining three traits were kept at their global mean values (Table 3).

294 To quantify any interaction between site productivity or disturbance regime on the one hand and
295 trait-related effects on the other, we repeated our analyses across a range of mean disturbance
296 intervals and site productivities.

297 # RESULTS

298 We first outline some general features of the model observed in a single-species stand with global
299 mean trait values. The purpose of this first section is to highlight how a size-structured model
300 naturally captures several known phenomena in vegetation dynamics. We then describe the
301 influence of the four traits on emergent properties of vegetation. In a final section, we briefly
302 investigate how trait-related shifts in vegetation could interact with shifts in site productivity or
303 disturbance regime.

304 ## GENERAL FEATURES OF THE MODEL

305 ### *COMPETITION FOR LIGHT LIMITS SEEDLING RECRUITMENT, SAPLING SURVIVAL, LAI,*
306 ### *AND DENSITY OF SEED RAIN*

307 Notwithstanding the continual influx of seeds, the model predicts several waves of recruitment and
308 a bimodal distribution of plant sizes during stand development (see central panel of Fig. 1). The first
309 wave of recruitment occurs immediately after disturbance, when individuals establish in open
310 conditions. Individuals at the top of the size hierarchy increase quickly in size and experience only
311 limited mortality. The growth of taller individuals decreases light available for individuals sitting
312 lower in the size hierarchy, reducing growth and increasing mortality. Declining light ultimately
313 limits seedling establishment. Eventually, however, enough individuals from the canopy die to

allow light at ground level to rise again above the minimum light requirement for seedlings. This initiates a second wave of recruitment, again followed by competitive thinning (Fig. 1). Competitive thinning operates such that individuals of a given size are removed at an increased rate while light levels are close or below their minimum light requirement. Since seedlings have the lowest burden of stem respiration per unit leaf area they are able to survive at lower light levels. As a result, competitive thinning constrains the LAI of whole stands to lie close to values corresponding to the minimum light requirement of seedlings.

Traditionally, self-thinning has been investigated by plotting average plant size (measured in leaf mass) against the number of individuals per area. A corresponding plot from our model is shown in Fig. 2. Following disturbance, the density of individuals and the LAI of the stand increase rapidly. Leaf area continues to accumulate until production from individuals at the bottom of the size hierarchy is close to zero. This is followed by a period of competitive thinning (from 1.4 – 13.8 years), during which average size increases and population density decreases (Fig. 2). The slope of this self-thinning trajectory is approximately -1.0, implying that the total mass of leaves remains nearly constant (but not exactly, as highlighted below). A second wave of seedling recruitment then moves the population back along the self-thinning trajectory towards smaller average size and larger density. The return trajectory in Fig. 2 is slightly offset from the initial trajectory, indicating that the actual density of leaf mass, and thus LAI, is not entirely fixed, instead varying slightly throughout stand development. These results are explained in more detail below.

Density-dependent growth within patches results in vegetation that is not seed-limited. The recruitment curve at landscape scale, i.e. integrated over all patch ages, shows that seed production is almost constant with respect to changes in seed rain (results not shown). This suggests that the emergent properties studied below will not differ substantially when mortality during dispersal is varied or when the assumption that metapopulations are demographically stable is relaxed.

AGE-RELATED DECLINES IN LAI AND NPP ARISE THROUGH COMPETITION, BUT ARE OFFSET BY SEEDLING RECRUITMENT

A plot of LAI against patch age shows how LAI first increases and then declines slightly before stabilising (Fig. 3), with NPP showing similar behaviour (results not shown). As outlined in the previous section, equilibrium LAI is mostly determined by the light requirement of seedlings, which accounts for its stabilising after the second wave of recruitment has been initiated. However, among individuals from the first wave of recruitment, the model predicts an age-related decline in LAI and NPP, as has been observed in numerous stands (see Ryan, Binkley, & Fownes 1997 and refs therein). The decline in LAI is caused by size-structured population dynamics, while increased stem respiration also contributes to the decline in NPP. To illustrate the mechanism of LAI decline, we have plotted LAI separately for three subsets of individuals based on the size distribution in older patches: 1) dominant individuals in the first wave of recruitment, which eventually form the canopy in older patches; 2) subordinates in the first wave of recruitment, which eventually die because they are competitively suppressed; and 3) all individuals in the second wave of recruitment (Fig. 3).

Among individuals in the first wave of recruitment, the initial decline in LAI after canopy closure (from 3.5 to 14.5 yrs) is due to mortality of competitively suppressed individuals (Fig. 3). During the first 5 years of stand development, the individuals that later become canopy dominants represent only a small fraction (in numbers and in leaf area) of all individuals in the first wave of recruitment (Fig. 3). However, these individuals have a small size advantage, which provides access to higher light and thus a growth advantage. As these dominant individuals increase in size, subordinate individuals become increasingly shaded, which increases mortality. A time lag occurs between the expansion of new leaves at the top of the canopy and the removal of shaded individuals at the bottom of the canopy. Consequently, LAI exceeds its sustainable value throughout the entire period during which canopy dominants continue to increase in size. This rise in LAI also explains the lack of seedling recruitment between 1.86 and 11.4 years.

A second phase of LAI decline (starting at 19.1 yrs) results from intrinsic mortality of canopy dominants after they have matured (Fig. 3). The competitive interactions leading to high mortality of subordinate individuals earlier during stand development means that there are few individuals available to replace the lost dominants, so the cumulative LAI of all individuals from the first wave of recruitment decreases. In our model, this second period of decline is compensated for by seedling recruitment, so the decline in LAI does not proceed beyond approximately 15 years. However, if data were reported only for large individuals (as would often be the case in forest surveys), or if recruitment were limited to periods immediately after disturbance, then a prolonged period of decline would be observed.

INFLUENCES OF TRAITS ON VEGETATION

Fig. 4 shows changes in the four vegetation properties during stand development following disturbance for low, average, and high settings of each trait, representing, respectively, the 5th, 50th, and 95th percentiles of empirically observed values. These temporal patterns were integrated over the patch-age distribution, to obtain a metapopulation average for each of the vegetation properties. Responses of these metapopulation averages to trait variation are summarised in Table 3. These responses are referred to as being small (< 10%), moderate (10-30%) or large (> 30%), according to the magnitude of change observed across the trait spectrum (see Table 3 for details). Fig. 5 gives a graphical depiction of the results for two of the four vegetation properties considered, under a range of disturbance regimes and productivities. Plots for the remaining vegetation properties, together with equilibrium seed rain, are included in Figs. S7 and S8.

RACE TO THE TOP: LEAF ECONOMICS, WOOD DENSITY, AND SEED SIZE ALL INFLUENCE HEIGHT GROWTH

Leaf economics, wood density, and seed size all influenced temporal patterns of height growth, while height at maturation had an effect on the eventual height of the canopy (Fig. 4). The influence of seed size on height growth was most intuitive: larger seeds resulted in larger seedlings, with this

size advantage being maintained until maturation. The influence of wood density on growth was also intuitive: lower wood density meant more economical stem construction, which in turn enables faster height growth. Note that wood density did not influence instantaneous dry-matter production in the model, but only the deployment of dry matter. Similarly, lower LMA conferred more economical leaf-area construction and thereby a faster growth rate, at least for smaller individuals. Since allocation to stem increased with size, the relative height advantage of low-wood-density strategies increased until maturation (Fig. 4). In contrast, the initial growth advantages of low LMA diminished over time, to the extent that high-LMA stands actually reached maturation size first, even though low LMA stands were initially the fastest growing (Fig. 4). This occurred because of an interaction between size and maximum growth rate. At small sizes, low LMA strategies have an advantage, because the benefits of cheaper leaf construction outweigh the costs of increased leaf turnover. At larger sizes, the opposite is true.

LAI IS INFLUENCED MORE BY MINIMUM LIGHT REQUIREMENT THAN BY INTRINSIC MORTALITY OR SEED RAIN

Leaf economics and height at maturation had a moderate influence on LAI, while wood density and seed size had only a small influence (Fig. 5; Table 3). The influence of leaf economics came about by altering the minimum light requirement of seedlings. Fast-growth strategies imply costs of increased leaf turnover and higher respiration rates per mass. The slope in the double logarithmic relationship between turnover rate and LMA was parameterised at -1.71 (see Appendix S7). A slope less than -1 means that decreases in the cost of deploying leaves (lower LMA) are associated with disproportionately larger increases in leaf turnover, leading to a greater light requirement for fast-growth strategies. The high light requirement of fast-growth strategies limited the sustainable LAI.

The influences of height at maturation, wood density and seed size were less intuitive. Height at maturation and seed size both influenced the density of seed rain (Table 3): height at maturation by diverting energy away from seed production, and seed size by altering the partitioning of mass

among offspring. Higher equilibrium seed rain increased rates of seedling germination, and even though most of the additional seedlings were thinned out through competitive interactions, there was a small to moderate increase in LAI (Fig. 5). Wood density also had a small effect on LAI because of influences on seedling mortality (Fig. 5).

HEIGHT AT MATURATION INFLUENCES NPP BY CHANGING THE TOTAL RESPIRATORY LOAD OF VEGETATION

Changes in NPP resulted from changes either in gross primary productivity (GPP), driven by total LAI, or in total respiration. Despite the influence of leaf economics on LAI (and therefore on GPP), leaf strategy caused no shift in NPP, because changes in GPP were compensated by changes in total stem and leaf respiration. The small changes in LAI driven by wood density and seed size translated into even smaller effects on NPP. However, the model assumed stem respiration was proportional to stem volume, and therefore, wood density affected NPP solely via mortality. It remains unclear if rates of stem respiration per volume vary with wood density, but if this were the case, some additional effect of wood density on NPP could be expected. Height at maturation, on the other hand, had a moderate effect on NPP, because taller stems had increased volumes of live sapwood and bark per individual.

TRAIT VARIATION OFFERS THREE ALTERNATIVE PATHWAYS TO INCREASED STANDING BIOMASS

Leaf economics, wood density, and height at maturation all led to large changes in biomass density (Fig. 5; Table 3), each realised through a different demographic pathway. Along the first pathway, leaf economic strategy altered leaf area and basal area. Increased LMA decreases the light requirement of individuals, causing an increase in population density, which in turn increases LAI and thus total sapwood volume. Additional wood mass accounted for most of the biomass change, but there was also a large (268%) change in total leaf mass associated with shifts in LMA. Along the second pathway, wood density shifted the allocation of mass between leaf and stem. Since wood density had only limited influence on LAI, similar total volumes of sapwood were maintained in

stands having low and high wood density. Stands with higher wood density therefore supported a greater standing mass of wood. Along the third pathway, height at maturation extended the growth period. By deferring the shift from vegetative to reproductive allocation, individuals accumulate more mass as wood.

LIMITED INFLUENCE OF SEED SIZE ON VEGETATION PROPERTIES

Changes in seed size had only small effects on LAI, NPP, and biomass density (Table 3), primarily because vegetation was not seed-limited. However, there were some noticeable effects of seed size on patterns of development in young stands (Fig. 4), and on average values for each of the vegetation properties in the metapopulation (Fig. 5). The influence of seed size on young stands had two parts. First, smaller seed size resulted in higher seed rain, which translated into faster increases in LAI and NPP after disturbance. LAI peaked earlier in stands with smaller seeds, and there was also a greater difference between peak and equilibrium LAI (Fig. 4). Second, larger seed size resulted in a height and biomass advantage that was maintained until reproduction. Because younger stands make up more than half the metapopulation, these transient effects of seed size, although small, did lead to changes in emergent vegetation properties of up to 15% (Table 3).

INFLUENCES OF DISTURBANCE REGIME AND SITE PRODUCTIVITY ON VEGETATION

Results presented above apply to stands growing under similar abiotic conditions. Here we investigate the sensitivity of these patterns to changes in site productivity and disturbance regime. While vegetation properties responded strongly to changes in productivity and disturbance, the influence of traits on vegetation dynamics was similar across the different stands (Fig. 5).

The strongest influence of disturbance interval was on average height and biomass; in contrast, LAI and NPP were almost constant for disturbance intervals longer than 15 years (Fig. 5a, Fig. S7). Height and biomass increased more slowly in developing stands than do NPP or LAI (Fig. 4). Shorter disturbance intervals decreased the fraction of the metapopulation at older stand ages;

464 therefore, landscape-wide biomass density and height were lower. At disturbance intervals of 15
465 years or less, LAI decreased strongly with height at maturation, because deferring seed production
466 to large sizes for short disturbance intervals generated chronically low reproductive output.
467 Realistically, species requiring large height at maturation would not persist under these conditions.

468 All four vegetation properties increased under more productive site conditions, as might be
469 expected (Fig. 5b, Fig. S8). The response of NPP to changes in site productivity was larger than to
470 trait variation, while for height, LAI, and biomass, the responses were similar in magnitude (Fig.
471 S8).

472 DISCUSSION

473 A primary challenge in modelling emergent properties of vegetation is to scale efficiently and
474 transparently from tissue-level, to individual-, population-, and landscape-level phenomena
475 (Prentice & Leemans 1990; Pacala et al. 1996; Levin et al. 1997; Moorcroft, Hurtt, and Pacala
476 2001). Ecological and life-history traits of individuals must have their influence on emergent
477 properties of vegetation via allocations among different tissue types and via the distributions of ages
478 and sizes. That is why the challenge must be approached with a model that incorporates the entire
479 life cycle of individuals, including the influences of traits, climate, competition, and disturbance on
480 demography and size structure. TSPMs (trait-size-patch-structured models) offer a viable
481 compromise between the detailed but noisy output of spatially explicit simulation models and the
482 convenience of modelling idealised stands lacking internal population structure. The TSPM
483 described here was used to investigate the influences of four functional traits, for which trade-offs
484 are relatively well understood, on several key properties of vegetation. The approach could be
485 extended to other traits, once the trade-offs governing their effects are sufficiently described.

THE DEMOGRAPHIC LINK BETWEEN TRAITS AND EMERGENT PROPERTIES OF VEGETATION

Leaf economic strategy had a moderate effect on LAI and a large effect on biomass density through a chain of influence that is well supported by empirical evidence. In the model, leaf strategy influenced LAI by altering plant light requirement (Givnish 1988; Baltzer & Thomas 2007). The relationship between LMA and turnover has a slope of less than -1 (Wright et al. 2004), meaning that fast growth strategies suffer from disproportionately fast turnover. Low-LMA strategies also imply higher respiration per unit leaf mass, because of higher nitrogen content per mass (Wright et al. 2004). High turnover and respiration increases the light requirement for individuals of a given size, which ultimately causes a decrease in LAI. Comparing single-species stands differing in leaf economic strategy, Reich et al. (1992) found a decrease in LAI and stand biomass, but no change in NPP, with shifts towards faster leaf strategy (lower LMA), which is consistent with our results. Beyond that, data from species-rich tropical forests support the influence of leaf economic strategy on minimum light requirement and on survival in low light (Condit, Hubbell, & Foster 1996; Poorter & Bongers 2006; Baltzer & Thomas 2007). Multi-species datasets also support the notion of faster initial height growth rates for low LMA strategies (Reich et al. 1992; Poorter & Bongers 2006).

The effect of leaf economic strategy on biomass density resulted from increasing the density of plants in the vegetation, whereas higher wood density and height at maturation increased the mass per individual. These effects are consistent with such stand-level data as are available. Baker et al. (2004) estimated that up to 40% of regional variation in above-ground mass for Amazonian tropical forests might be attributed to differences in wood density. Keith, Mackey, and Lindenmayer (2009) found that the world's tallest forests also contain the greatest mass of carbon. Furthermore, our model indicates that trait variation may increase biomass density without increasing NPP. In fact, NPP decreased slightly in taller stands because of additional stem respiration. Wood density had a negligible influence on NPP, in line with theoretical expectations (Enquist et al. 1999), but this

result hinges on our assumption of constant stem respiration per volume. If rates of stem respiration per volume were found to increase with wood density, then NPP would decrease. So what are plants sacrificing to achieve this additional expenditure on stem tissues in high wood density and tall stands? In the case of height at maturation, additional stem mass came at the expense of reproductive output. In the case of wood density, high-density stands have less intrinsic mortality, decreasing the rate at which accumulated carbon is recycled into the litter pool.

Biomass density was the vegetation property we found to be most sensitive to trait variation and changes in disturbance frequency. Other studies have likewise reported a large influence of disturbance regime on standing biomass. For example, Hurtt et al. (2002) used a PDE-based model to estimate historical patterns of carbon flux resulting from land-use change in North America. They estimated that early land-use changes, mainly clearing for agriculture, caused a net efflux of carbon from terrestrial ecosystems, while fire suppression and agricultural abandonment since 1900 have resulted in a net uptake of carbon throughout the 20th century. The advantage of using a TSPM to estimate landscape-scale changes in biomass is that rates of change are directly constrained by current patch structure and size structure. In this context, it is interesting to note that most DGVMs, as well as land-surface models coupled with global climate models, do not explicitly consider patch structure or size structure (Cramer et al. 2001; Bonan & Levis 2002; Sitch et al. 2008). While these models may prove accurate in predicting NPP, which we found to be relatively insensitive to traits and disturbance regime, their predictions about biomass density may be less informative than those coming from a TSPM in which patch age and stand structure are explicitly modelled.

Combined, our results underscore the need for vegetation models to incorporate functional traits together with their effects on the patch structure and size structure of vegetation. Our study has shown that the effects of some traits on vegetation properties may be as strong as the influence of site productivity and disturbance, although it should be noted that these predictions have been

derived for single-species stands only. The ecological dynamics that give rise to these effects also illustrate why size structure within populations is important. Size structure was present in the stochastic gap models widely used during the past three decades (for reviews, see Shugart 1984; Bugmann 2001). However, stochastic simulators inhibit detailed investigations of ecological feedbacks such as those presented here, and are not practical for incorporation into large-scale applications like DGVMs. For these reasons, researchers have sought ways to approximate the collective dynamics of heterogeneous populations (Sinko & Streifer 1967; Levin & Paine 1974; Metz & Diekmann 1986; Levin et al. 1997; de Roos 1997), leading to the development of PDE-based models (Kohyama 1993; Moorcroft, Hurtt, and Pacala 2001; Strigul et al. 2008; Medvigy et al. 2009). Since PDE-based models can account for patch and size structure, while enabling deterministic numerical solutions, they have been advocated as a possible foundation for next-generation DGVMs (Purves & Pacala 2008).

IMPLICATIONS FOR MULTI-SPECIES STANDS

For the most part, we expect the results presented here to extend to multi-species stands. Patch- and size-structured models, formulated either as stochastic gap-models or as their deterministic approximations, can easily accommodate multiple species, provided there is an opportunity for the different types to coexist (Shugart 1984; Kohyama 1993). These models are thus well suited for investigating questions about community assembly and the effects of species diversity on ecosystem function. Based on the results presented here, we predict that the LAI of multi-species stands will be determined mainly by the species with highest LMA, since leaf area will continue to accumulate while light levels remain above that species' light requirement. To the extent they are influenced by LAI, NPP and biomass density may exhibit similar patterns. However, these vegetation properties are also influenced by wood density and height at maturation, whose influence on multi-species stands will be determined by the precise mixture of trait values rather than by the most extreme trait value. Shifts in the average trait value are bound to produce a corresponding shift in emergent

properties. Quantifying these effects in the field may be complicated by the known covariation of traits with climate and other site factors: leaf economic strategy and wood density move towards faster growth, and height and seed mass increase, as abiotic conditions become more favourable for growth (Wright et al. 2004; Moles et al. 2005, 2009; Chave et al. 2009). This suggests a key role for TSPMs in assessing how climate and traits combine to give rise to variation in vegetation properties across landscapes.

FURTHER REFINING THE REPRESENTATION OF VEGETATION IN TSPMS

The representation of vegetation in current TSPMs is an improvement over most DGVMs, which lack internal population and patch structure (see also Moorcroft, Hurtt, and Pacala 2001; Hurtt et al. 2002; Medvigy et al. 2009). Nevertheless, this representation remains a simplified version of real communities. It is therefore worth noting some outstanding challenges for the TSPM approach.

Probably the most significant challenge is to determine whether a single state dimension adequately describes the ontogenetic pathway traversed by individuals within a species as they mature. With a single state dimension, the various size metrics that describe individuals within a species, such as crown leaf area, height, stem basal area, or root mass have to be bound together, so that all size metrics can be predicted from a single variable. This means that allocation, for example to roots versus leaves, cannot change dynamically in response to environmental conditions, except by varying the traits of the entire species (i.e. by redefining the ontogenetic pathway). In principle, more state dimensions can be included (e.g. Moorcroft, Hurtt, and Pacala 2001), but this makes the model harder to solve. In contrast, most DGVMs maintain numerous state dimensions, but to make this possible, they sacrifice all detail regarding size structure within each species, so that the entire metapopulation of a species is represented in terms of a single average-sized individual, with recruits also entering at this size (Cramer et al. 2001; Bonan & Levis 2002; Woodward & Lomas 2004; Sitch et al. 2008). While it will be worthwhile to attempt implementing extensions of the

586 TSPM approach presented here to multiple state dimensions, so far stochastic simulations are
587 offering the only practical way to combine multiple state dimensions with detailed size structure.

588 The assumption that disturbances are stand-replacing may also be cause for concern. This
589 assumption makes it easier to scale up from a single patch to the entire metapopulation. But in many
590 cases, disturbances remove only part of a patch's vegetation, resulting in a complex age structure
591 within each patch (Pickett & White 1985). To properly incorporate these dynamics would be
592 computationally challenging, since each patch in the metapopulation would need to be simulated
593 explicitly. The question thus remains how much this refinement would influence our results.
594 However, there are vegetation types for which the stand-replacement assumption applies (Pickett &
595 White 1985; Clark 1989; Coomes & Allen 2007), making it a reasonable first approximation of
596 disturbance-driven vegetation dynamics.

597 An even broader challenge is to determine how well the PDEs used in TSPMs approximate
598 competitive and disturbance-driven vegetation dynamics. The PDE governing stand development
599 used here has been derived both as the deterministic limit for increasingly large patches (Kohyama
600 1993; de Roos 1997), and as the average of many runs of a stochastic gap model containing few
601 individuals per patch (Moorcroft, Hurtt, and Pacala 2001). This suggests that the PDE may suit a
602 variety of disturbance types, although both derivations assume spatial homogeneity within patches.
603 Including spatial interactions within patches could, in principle, alter patterns of stand development,
604 although the effect on the emergent properties considered here might be minimal (Busing & Mailly
605 2004). For example, Strigul et al. (2008) showed that when phototropic effects were included in
606 spatial simulations of stand development, basal area and tree density were well approximated by the
607 standard PDE used here, which ignores within-patch spatial effects (see also Hurtt et al. 1998).
608 Likewise, accounting for the distribution of patch ages across a landscape may be sufficient for
609 estimating emergent properties of metapopulations, without considering the spatial arrangement of
610 patches. More generally, the approach of modelling a dynamic landscape, in which individual

patches constantly change, within an equilibrium framework seems promising for reconciling "equilibrium" and "non-equilibrium" approaches to modelling ecological dynamics (Levin & Paine 1974; Connell 1978; Bormann & Likens 1979).

A NECESSARY BUT DIFFICULT CHALLENGE: CONFIRMING MODEL PREDICTIONS

As vegetation models become more complex they may account for an increasing array of observable phenomena. However, our ability to confirm the behaviour of sophisticated models has been limited by the availability of suitable data. For example, we found only a single data set relating trait values to emergent properties of vegetation in single-species forest stands (Reich et al. 1992). Other data sets exist for traits, for ecosystem properties, and for stand structure, but these are almost always disconnected from one another, which is far from ideal. There is also a shortage of adequate data with which to parameterise and test the various sub-models in TSPMs. To parameterise our model we have drawn on some of the best data sources available, but still they are not ideal, and also they come from a mixture of situations. Consider the Coweeta dataset (Martin et al. 1998) used to parameterise our allocation model. It provides unusually good within-species resolution, but even so, the dataset is limited to relatively large trees so our estimates of sapling allometry are rough approximations at best. It is also unclear how representative these allometries are of other vegetation types. The general problem is that researchers have thus far relied on a disparate range of data sources of varying quality for model parameterisation and confirmation, as have we.

We are optimistic about future opportunities for fruitful model-data comparisons. Long-term records of size-structured growth dynamics are accumulating for a variety of sites, and in some cases, are being supplemented with species trait data (e.g. Wright et al. 2010). Such data will offer unparalleled opportunities to evaluate the performance of TSPMs (Purves & Pacala 2008; Medvigy et al. 2009). Importantly, detailed datasets allow TSPMs to be evaluated based on their ability to

predict multiple phenomena, whereas previous research has focussed on individual phenomena in isolation. Combined with detailed records from ecosystem flux towers, long-term plot data also offer a pathway for refining weakly constrained model parameters (Medvigy et al. 2009). There also exist many experimental plantings worldwide established by forestry services, offering a rich source of potential data if it can be accessed. Overall, certainty in model predictions would be improved through collation and assimilation of standardised datasets from a variety of species and systems.

CONCLUSIONS

To investigate the impact of LMA, wood density, seed size, and height at maturation on emergent properties of vegetation, we used a model capturing the entire life cycle of individuals, from germination to sapling growth and maturation, because the advantages of these traits are manifested through influences on size distribution and demography. In the past, individual-based models have often relied on empirically motivated growth equations (e.g. Shugart 1984; Pacala et al. 1996; Bugmann 2001). However, growth is an outcome of traits operating in a given environment, and the model presented here captures physiological processes and generates many aspects of individual performance, stand dynamics, and properties of vegetation from trait variation (see also Friend et al. 1997; Moorcroft, Hurtt, and Pacala 2001). Trait-based models are also easier to calibrate for new sites and species mixtures. It is therefore hoped that the framework we have presented here may open up new avenues for understanding the role of traits in structuring vegetation through physiological, ecological, and evolutionary processes.

ACKNOWLEDGEMENTS

This work has been supported by funding from the Australian Research Council, the International Institute for Applied Systems Analysis, Macquarie University, the Swedish Research Council, and Umeå University. We thank J. Johansson, C. Lusk, A. de Roos and three anonymous reviewers for comments on earlier versions of this paper, and B. Medlyn, I. C. Prentice, and P. Reich for valuable discussions.

REFERENCES

Baker, T.R., Phillips, O.L., Malhi, Y., Almeida, S., Arroyo, L., Di Fiore, A., Erwin, T., Killeen, T.J., Laurance, S.G., Laurance, W.F., Lewis, S.L., Lloyd, J., Monteagudo, A., Neill, D.A., Patiño, S., Pitman, N.C.A., Silva, J.N.M. & Martinez, R.V. (2004) Variation in wood density determines spatial patterns in Amazonian forest biomass. *Global Change Biology*, **10**, 545-562.

Baltzer, J.L. & Thomas, S.C. (2007) Determinants of whole-plant light requirements in Bornean rain forest tree saplings. *Journal of Ecology*, **95**, 1208-1221.

Bonan, G. & Levis, S. (2002) Landscapes as patches of plant functional types: an integrating concept for climate and ecosystem models. *Global Biogeochemical Cycles*, **16**, 1021.

Bonan, G.B. (2008) Forests and climate change: forcings, feedbacks, and the climate benefits of forests. *Science*, **320**, 1444-1449.

Bormann, F.H. & Likens, G.E. (1979) Catastrophic disturbance and the steady state in northern hardwood forests. *American Scientist*, **67**, 660-669.

Bugmann, H. (2001) A review of forest gap models. *Climatic Change*, **51**, 259-305.

Busing, R.T. & Mailly, D. (2004) Advances in spatial, individual-based modelling of forest dynamics. *Journal of Vegetation Science*, **15**, 831.

Cannell, M.G.R. & Thornley, J.H.M. (1998) Temperature and CO[2] responses of leaf and canopy photosynthesis: a clarification using the non-rectangular hyperbola model of photosynthesis. *Annals of Botany*, **82**, 883-892.

Chave, J., Coomes, D.A., Jansen,, S., Lewis, S.L., Swenson, N.G. & Zanne, A. (2009) Towards a worldwide wood economics spectrum. *Ecology Letters*, **12**, 351-366.

683 Clark, J.S. (1989) Ecological disturbance as a renewal process: theory and application to fire
684 history. *Oikos*, **56**, 17-30.

685 Condit, R., Hubbell, S.P. & Foster, R.B. (1996) Assessing the response of plant functional types to
686 climate change in tropical forests. *Journal of Vegetation Science*, **7**, 405-416.

687 Connell, J.H. (1978) Diversity in tropical rain forests and coral reefs. *Science*, **199**, 1302-1310.

688 Coomes, D.A. & Allen, R.B. (2007) Mortality and tree-size distributions in natural mixed-age
689 forests. *Journal of Ecology*, **95**, 27-40.

690 Cramer, W., Bondeau, A., Woodward, F.I., Prentice, I.C., Betts, R.A., Brovkin, V., Cox, P.M.,
691 Fisher, V., Foley, J.A., Friend, A.D., Kucharik, C., Lomas, M.R., Ramankutty, N., Sitch, S.,
692 Smith, B., White, A. & Young-Molling, C. (2001) Global response of terrestrial ecosystem
693 structure and function to CO2 and climate change: results from six dynamic global
694 vegetation models. *Global Change Biology*, **7**, 357-373.

695 Enquist, B.J., West, G.B., Charnov, E.L. & Brown, J.H. (1999) Allometric scaling of production
696 and life-history variation in vascular plants. *Nature*, **401**, 907-911.

697 Friend, A.D., Stevens, A.K., Knox, R. & Cannell, M.G.R. (1997) A process-based, terrestrial
698 biosphere model of ecosystem dynamics (Hybrid v3.0). *Ecological Modelling*, **95**, 249-287.

699 Givnish, T.J. (1988) Adaptation to sun and shade: a whole-plant perspective. *Australian Journal of*
700 *Plant Physiology*, **15**, 63-92.

701 Goff, F.G. & West, D. (1975) Canopy-understory interaction effects on forest population structure.
702 *Forest Science*, **21**, 98-108.

703 Hara, T. (1984) A stochastic model and the moment dynamics of the growth and size distribution of

plant populations. *Journal of Theoretical Biology*, **109**, 173-190.

Hector, A. & Bagchi, R. (2007) Biodiversity and ecosystem multifunctionality. *Nature*, **448**, 188-190.

Hooper, D.U., Chapin, F.S., Ewel, J.J., Hector, A., Inchausti, P., Lavorel, S., Lawton, J.H., Lodge, D.M., Loreau, M., Naeem, S., Schmid, B., Setälä, H., Symstad, A.J., Vandermeer, J. & Wardle, D.A. (2005) Effects of biodiversity on ecosystem functioning: a consensus of current knowledge. *Ecological Monographs*, **75**, 3-35.

Hurtt, G.C., Moorcroft, P.R., Pacala, S.W. & Levin, S.A. (1998) Terrestrial models and global change: challenges for the future. *Global Change Biology*, **4**, 581-590.

Hurtt, G.C., Pacala, S.W., Moorcroft, P.R., Caspersen, J., Shevliakova, E., Houghton, R.A. & Moore, B. (2002) Projecting the future of the U.S. carbon sink. *Proceedings of the National Academy of Sciences, USA*, **99**, 1389-1394.

Huston, M. & Smith, T. (1987) Plant succession: life history and competition. *American Naturalist*, **130**, 168-198.

Huston, M.A. & DeAngelis, D.L. (1987) Size bimodality in monospecific populations: a critical review of potential mechanisms. *American Naturalist*, **129**, 678-707.

Iwasa, Y. (2000) Dynamic optimization of plant growth. *Evolutionary Ecology Research*, **2**, 437-455.

Keith, H., Mackey, B.G. & Lindenmayer, D.B. (2009) Re-evaluation of forest biomass carbon stocks and lessons from the world's most carbon-dense forests. *Proceedings of the National Academy of Sciences, USA*, in press.

725 King, D.A., Davies, S.J., Tan, S. & Noor, N.S.M. (2006) The role of wood density and stem support
726 costs in the growth and mortality of tropical trees. *Journal of Ecology*, **94**, 670-680.

727 Kohyama, T. (1993) Size-structured tree populations in gap-dynamic forest: the forest architecture
728 hypothesis for the stable coexistence of species. *Journal of Ecology*, **81**, 131-143.

729 Levin, S.A., Grenfell, B., Hastings, A. & Perelson, A.S. (1997) Mathematical and computational
730 challenges in population biology and ecosystems science. *Science*, **275**, 334-343.

731 Levin, S.A. & Paine, R.T. (1974) Disturbance, patch formation, and community structure.
732 *Proceedings of the National Academy of Sciences, USA*, **71**, 2744-2747.

733 Martin, J.G., Kloeppel, B.D., Schaefer, T.L., Kimbler, D.L. & McNulty, S.G. (1998) Aboveground
734 biomass and nitrogen allocation of ten deciduous southern Appalachian tree species.
735 *Canadian Journal of Forest Research*, **28**, 1648-1658.

736 Mäkelä, A. (1985) Differential games in evolutionary theory: height growth strategies of trees.
737 *Theoretical Population Biology*, **27**, 239-267.

738 McCarthy, M.A., Gill, A.M. & Bradstock, R.A. (2001) Theoretical fire-interval distributions.
739 *International Journal of Wildland Fire*, **10**, 73-77.

740 Medvigy, D., Wofsy, S.C., Munger, J.W., Hollinger, D.Y. & Moorcroft, P.R. (2009) Mechanistic
741 scaling of ecosystem function and dynamics in space and time: Ecosystem Demography
742 model version 2. *Journal of Geophysical Research*, **114**, G01002.

743 Metz, J.A.J. & Diekmann, O. (1986) The dynamics of physiologically structured populations.
744 *Lecture notes in biomathematics*, **68**.

745 Moles, A.T., Ackerly, D.D., Webb, C.O., Tweddle, J.C., Dickie, J.B., Pitman, A.J. & Westoby, M.

(2005) Factors that shape seed mass evolution. *Proceedings of the National Academy of Science, USA*, **102**, 10540-10544.

Moles, A.T., Falster, D.S., Leishman, M. & Westoby, M. (2004) Small-seeded plants produce more seeds per square metre of canopy per year, but not per individual per lifetime. *Journal of Ecology*, **92**, 384–396.

Moles, A.T., Warton, D.I., Warman, L., Swenson, N.G., Laffan, S.W., Zanne, A.E., Pitman, A., Hemmings, F.A. & Leishman, M.R. (2009) Global patterns in plant height. *Journal of Ecology*, **97**, 923 - 932.

Moorcroft, P.R., Hurtt, G.C. & Pacala, S.W. (2001) A method for scaling vegetation dynamics: the ecosystem demography model (ED). *Ecological Monographs*, **71**, 557-585.

Muller-Landau, H.C. (2004) Interspecific and inter-site variation in wood specific gravity of tropical trees. *Biotropica*, **36**, 20-32.

Pacala, S.W., Canham, C.D., Saponara, J., Silander, J.A., Kobe, R.K. & Ribbens, E. (1996) Forest models defined by field measurements - estimation, error analysis and dynamics. *Ecological Monographs*, **66**, 1-43.

Pickett, S.T.A. & White, P.S. (1985) *The ecology of natural disturbance and patch dynamics*. Academic Press.

Poorter, L. & Bongers, F. (2006) Leaf traits are good predictors of plant performance across 53 rain forest species. *Ecology*, **87**, 1733-1743.

Prentice, I. & Leemans, R. (1990) Pattern and process and the dynamics of forest structure: A simulation approach. *Journal of Ecology*, **78**, 340-355.

767 Press, W.H. (1995) *Numerical recipes in C: the art of scientific computing*. Cambridge University
768 Press, Cambridge ; New York.

769 Purves, D. & Pacala, S. (2008) Predictive models of forest dynamics. *Science*, **320**, 1452-1453.

770 Reich, P.B., Walters, M.B. & Ellsworth, D.S. (1992) Leaf life-span in relation to leaf, plant, and
771 stand characteristics among diverse ecosystems. *Ecological Monographs*, **62**, 365-392.

772 de Roos, A.M. (1997) A gentle introduction to physiologically structured population models.
773 *Structured population models in marine, terrestrial and fresh-water systems*. pp. 119-204.
774 Chapman & Hall, New York.

775 Ryan, M.G., Binkley, D. & Fownes, J.H. (1997) Age-related decline in forest productivity: pattern
776 and process. *Advances in Ecological Research*, **27**, 213-262.

777 Shinozaki, K., Yoda, K., Hozumi, K. & Kira, T. (1964) A quantitative analysis of plant form - the
778 pipe model theory. I. Basic analyses. *Japanese Journal of Ecology*, **14**, 97-105.

779 Shugart, H.H. (1984) *A theory of forest dynamics: the ecological implications of forest succession*.
780 Springer-Verlag, New York.

781 Shukla, J. & Mintz, Y. (1982) Influence of land-surface evapotranspiration on the earth's climate.
782 *Science*, **215**, 1498-1501.

783 Sinko, J.W. & Streifer, W. (1967) A new model for age-size structure of a population. *Ecology*, **48**,
784 910-918.

785 Sitch, S., Huntingford, C., Gedney, N., Levy, P.E., Lomas, M., Piao, S.L., Betts, R., Ciais, P., Cox,
786 P., Friedlingstein, P., Jones, C.D., Prentice, I.C. & Woodward, F.I. (2008) Evaluation of the
787 terrestrial carbon cycle, future plant geography and climate-carbon cycle feedbacks using

five Dynamic Global Vegetation Models (DGVMs). *Global Change Biology*, **14**, 2015-2039.

Strigul, N., Pristinski, D., Purves, D., Dushoff, J. & Pacala, S. (2008) Scaling from trees to forests: tractable macroscopic equations for forest dynamics. *Ecological Monographs*, **78**, 523-545.

Tilman, D., Knops, J., Wedin, D., Reich, P., Ritchie, M. & Siemann, E. (1997) The influence of functional diversity and composition on ecosystem processes. *Science*, **277**, 1300-1302.

Westoby, M., Falster, D.S., Moles, A.T., Vesk, P. & Wright, I.J. (2002) Plant ecological strategies: some leading dimensions of variation between species. *Annual Review of Ecology and Systematics*, **33**, 125-159.

Woodward, F.I. & Lomas, M.R. (2004) Vegetation dynamics - simulating responses to climatic change. *Biological Reviews*, **79**, 643-670.

Wright, I.J., Reich, P.B., Westoby, M., Ackerly, D., Baruch, Z., Bongers, F., Cavender-Bares, J., Chapin, F., Cornelissen, J., Diemer, M., Flexas, J., Garnier, E., Groom, P., Gulias, J., Hikosaka, K., Lamont, B., Lee, T., Lee, W., Lusk, C., Midgley, J., Navas, M., Niinemets, Ü., Oleksyn, J., Osada, N., Poorter, H., Poot, P., Prior, L., Pyankov, V., Roumet, C., Thomas, S., Tjoelker, M., Veneklaas, E. & Villar, R. (2004) The world-wide leaf economics spectrum. *Nature*, **428**, 821-827.

Wright, S.J., Kitajima, K., Kraft, N., Reich, P., Wright, I., Bunker, D., Condit, R., Dalling, J., Davies, S., Diaz, S., Engelbrecht, B., Harms, K., Hubbell, S., Marks, C., Ruiz-Jaen, M., Salvador, C. & Zanne, A. (2010) Functional traits and the growth-mortality tradeoff in tropical trees. *Ecology*, 100621220348088.

Yokozawa, M. & Hara, T. (1992) A canopy photosynthesis model for the dynamics of size structure

and self-thinning in plant-populations. *Annals of Botany*, **70**, 305-316.

Yokozawa, M. & Hara, T. (1995) Foliage profile, size structure and stem diameter plant height relationship in crowded plant-populations. *Annals of Botany*, **76**, 271-285.

Zanne, A., Lopez-Gonzalez, G., Coomes, D.A., Ilic, J., Jansen, S., Lewis, S.L., Miller, R.B., Swenson, N.G., Wiemann, M.C. & Chave, J. (2009) Global wood density database. *Global wood density database. Dryad. Identifier: http://hdl.handle.net/10255/dryad.235.*

SUPPORTING INFORMATION

Additional supporting information may be found in the online version of this article:

Appendix S1 Derivation of equilibrium patch-age distribution

Appendix S2 Derivation of biomass-allocation model

Appendix S3 Confirmation of biomass-allocation model

Appendix S4 Relationship between mortality and wood density

Appendix S5 Derivation of seedling germination-survival model

Appendix S6 Calculation of gross annual assimilation from solar patterns

Appendix S7 Model calibration

Table S1 Tests of model assumptions and derived trait values for individuals from 10 species contained in the Coweeta biomass dataset.

Figure S1 Equilibrium density distribution of patch ages in relation mean disturbance interval .

Figure S2 Observed relationships between (a) leaf area and sapwood area, (b) leaf area and height, and (c) leaf area and heartwood volume in the Coweeta biomass data.

Figure S3 Predicted and observed values for (a) sapwood mass and (b) bark mass in the Coweeta biomass data.

Figure S4 Relationship between wood density and log-transformed mortality rate at four sites.

Figure S5 Instantaneous (a) and annual (b) photosynthetic light response curves with nitrogen use efficiency set at different values.

Figure S6 Influence of plant size on allocation and dry mass production.

836 Figure S7 Dependence of emergent properties of vegetation and equilibrium seed rain on trait
837 values, for metapopulations with different mean interval between disturbances.

838 Figure S8 Dependence of emergent properties of vegetation and equilibrium seed rain on trait
839 values, for metapopulations with different productivity.

840

841

Table 1 Model variables and equations. For the sake of brevity, dependencies of functions are shown only in the Symbol column. The variable x refers to a vector of four traits that are varied in the model: $x = (\phi, \rho, h_m, s)$. Subscripts for size variables are: l = leaves, s = sapwood, b = bark and phloem, h = heartwood, r = fine roots. All mass measurements are in terms of dry mass.

Variable	Symbol	Unit	Determination	Equation
Traits				
Leaf mass per unit area (LMA)	ϕ	kg m^{-2}		
Stem tissue density	ρ	kg m^{-3}		
Height at maturation	h_m	m		
Seed size*	s	kg	$m_t(x, m_{l,0}) = s$	1
Individual size				
Mass of leaves	m_l	kg		
Leaf area	$\omega(x, m_l)$	m^2	$\omega = m_l \phi^{-1}$	2
Height	$h(x, m_l)$	m	$h = \alpha_1 \omega(x, m_l)^{\beta_1}$	3
Mass of sapwood	$m_s(x, m_l)$	kg	$m_s = \rho \eta_c \theta^{-1} \omega(x, m_l) h(x, m_l)$	4
Mass of bark	$m_b(x, m_l)$	kg	$m_b = b m_s(x, m_l)$	5
Mass of heartwood	$m_h(x, m_l)$	kg	$m_h = \rho \eta_c \alpha_2 \omega(x, m_l)^{\beta_2}$	6
Mass of fine roots	$m_r(x, m_l)$	kg	$m_r = \alpha_3 \omega(x, m_l)$	7
Total mass	$m_t(x, m_l)$	kg	$m_t = m_l + m_s + m_b + m_h + m_r$	8
Competitive environment				
Probability density of leaf area at height z for an individual of height h	$q(z,h)$	m^{-1}	$q = 2\eta\left(1 - z^\eta h^{-\eta}\right) z^{\eta-1} h^{-\eta}$ if $z \le h$, otherwise 0	9
Fraction of leaf area above height z for an individual of height h	$Q(z,h)$	dimensionless (0 to 1)	$Q = \int_z^h q(z', h)\, \mathrm{d}z'$ if $z \le h$, otherwise 0	10
Canopy openness at height z in a patch of age a	$E(z,a)$	dimensionless (0 to 1)	$E = \exp\left(-c_{ext} \int_0^\infty Q(z, h(m_l)) \omega(x, m_l) n(x, m_l, a)\, \mathrm{d}m_l\right)$	11
Mass production†				
Gross annual CO_2 assimilation‡	$A(x, m_l, E(\cdot, a))$	mol yr^{-1}	$A = \omega(x, m_l) \int_0^{h(m_l)} A_{lf}(A_0 v, E(z,a)) q(z, h(m_l))\, \mathrm{d}z$	12

Total maintenance respiration	$R(x,m_l)$	mol yr^{-1}	$R = \omega(x,m_l)\left(c_{R,l} + \frac{m_s(x,m_l) + 2m_b(x,m_l)}{\rho} c_{R,s} + m_r(x,m_l) c_{R,r}\right)$	13
Total turnover	$T(x,m_l)$	kg yr^{-1}	$T = m_l\left(\alpha_4 \phi^{-B_4}\right) + m_b(x,m_l) k_b + m_r(x,m_l) k_r$	14
Net production	$P(x,m_l,E(\cdot,a))$	kg yr^{-1}	$P = c_{bio} Y \left[A(x,m_l,E(\cdot,a)) - R(x,m_l)\right] - T(x,m_l)$	15
Fraction of production allocated to reproduction	$r(x,m_l)$	dimensionless (0 to 1)	$r = c_{r1}\left(1 + \exp\left(c_{r2}\left(1 - \frac{h(x,m_l)}{h_m}\right)\right)\right)^{-1}$	16
Rate of offspring production	$f(x,m_l,E(\cdot,a))$	yr^{-1}	$f = r(x,m_l) P(x,m_l,E(\cdot,a)) / (c_{acc} s)$ if $P(x,m_{l,0},E(\cdot,a)) > 0$, otherwise 0	17
Fraction of whole-plant growth that is leaf¶	$\frac{dm_l}{dm_t}(x,m_l)$	dimensionless (0 to 1)	$\frac{dm_l}{dm_t} = \left(1 + \frac{dm_s}{dm_l}(x,m_l) + \frac{dm_b}{dm_l}(x,m_l) + \frac{dm_h}{dm_l}(x,m_l) + \frac{dm_r}{dm_l}(x,m_l)\right)^{-1}$	18
Growth rate in leaf mass	$g(x,m_l,E(\cdot,a))$	kg yr^{-1}	$g = (1 - r(x,m_l)) P(x,m_l,E(\cdot,a)) \frac{dm_l}{dm_t}(x,m_l)$ if $P(x,m_{l,0},E(\cdot,a)) > 0$, otherwise 0	19
Mortality				
Survival of seedlings during germination	$\pi_1(x,m_0,E(\cdot,a))$	dimensionless (0 to 1)	$\pi_1 = \left(\left(\frac{P(x,m_{l,0},E(\cdot,a))}{\omega(x,m_{l,0})}\right)^{-2} c_{s0}^{\,2} + 1\right)^{-1}$ if $P(x,m_{l,0},E(\cdot,a)) > 0$, otherwise 0	20
Instantaneous mortality rate	$d(x,m_l,E(\cdot,a))$	yr^{-1}	$d = c_{d0}\exp(-c_{d1}\rho) + c_{d2}\exp\left(-c_{d3}\left(\frac{P(x,m_l,E(\cdot,a))}{\omega(x,m_l)}\right)\right)$	21
Development of size distribution within patches				
Density per ground area of individuals with traits x and size m_l in a patch of age a	$n(x,m_l,a)$	kg^{-1} m^{-2}	$\frac{\partial}{\partial a} n(x,m_l,a) = -d(x,m_l,E(\cdot,a)) n(x,m_l,a) - \frac{\partial}{\partial m_l}\left[g(x,m_l,E(\cdot,a)) n(x,m_l,a)\right]$ $n(x,m_l,0) = 0,$ $n(x,m_{l,0},a) = \frac{\pi_1(x,m_{l,0},E(\cdot,a))}{g(x,m_{l,0},E(\cdot,a))} \int_0^\infty p(\tau) \int_0^\infty \pi_0 f(x,m_l,E(\cdot,\tau)) n(x,m_l,\tau)\,dm_l\,d\tau$ if $P(x,m_{l,0},E(\cdot,a)) > 0$, otherwise 0	22
Metapopulation dynamics				
Probability density of patch age a in the metapopulation§	$p(a)$	yr^{-1}	$p = \frac{1}{\hat{a}} \exp\left(-\frac{\pi}{4}\left(\frac{a}{\hat{a}}\right)^2\right)$	23
Emergent properties of vegetation*				
Average height of leaf area	$H(a)$	m	$H = \frac{1}{L(a)} \int_0^\infty \int_0^\infty \omega(x,m_l) q(z,h(x,m_l)) n(x,m_l,a) h(x,m_l)\,dm_l\,dz$	24
Leaf-area index	$L(a)$	dimensionless	$L = \int_0^\infty \omega(x,m_l) n(x,m_l,a)\,dm_l$	25

Net primary production	$N(a)$	kg m^{-2} yr^{-1}	$\mathrm{N} = c_{\mathrm{bio}} Y \int_0^\infty \left[A\left(x, m_1, E(\cdot, a)\right) - R(x, m_1)\right] n(x, m_1, a)\, \mathrm{d}m_1$	26
Biomass density	$B(a)$	kg m^{-2}	$\mathrm{B} = \int_0^\infty m_t(m_1)\, n(x, m_1, a)\, \mathrm{d}m_1$	27

* Leaf mass at germination, $m_{l,0}$, is obtained by finding a value that satisfies equation 1 and varies as a function of ϕ, ρ and s.

† All rates are per plant.

‡ $A_{\mathrm{lf}}\left(A_0 \upsilon, E(z,a)\right)$ is the gross annual CO_2 assimilation per unit leaf area at canopy openness $E(z,a)$ for a leaf with maximum capacity $A_0 \upsilon$, determined by integrating instantaneous rates of assimilation (described by a rectangular hyperbola) over the diurnal solar cycles throughout the year. For details see Appendix S6.

¶ The derivatives on the right-hand side of eqn 18 can be calculated directly from eqn 4-7. For solutions see Appendix S2.

§ $\hat{a}$ is the mean interval between disturbances. The probability of patch disturbance is assumed to increase linearly with patch age, and can be expressed as a function of mean disturbance interval, $\gamma(a) = \frac{\pi a}{2\hat{a}^2}$. For more details see Appendix S1.

** Averages over all patches in the metapopulation, calculated as $\int_0^\infty p(a) K(a)\, \mathrm{d}a$, where $K(a)$ is the considered vegetation property at patch age a.

Table 2 Model parameters. Corresponding equations in Table 1 are indicated. Sources: (1) estimate from Coweeta dataset (Martin et al. 1998), (2) arbitrary assumption, (3) see Appendix S7.

Description	Symbol	Unit	Value	Source	Equation
Competitive interactions					
Light-extinction coefficient	c_{ext}	dimensionless (0 to 1)	0.5	3	11
Individual allometry					
Crown-shape parameter	η	dimensionless	12	2	9
Stem-volume adjustment due to crown shape	η_{c}	dimensionless (0 to 1)	$1-\frac{2}{1+\eta}+\frac{1}{1+2\eta}$	-	4-6, 18
Leaf area per sapwood area	θ	dimensionless	4669	1	4-5,18
Parameters describing scaling of height with leaf area	α_1,β_1	m^{-1}, dimensionless	5.44, 0.306	1	3-5,18
Parameters describing scaling of heartwood volume with leaf area	α_2,β_2	m, dimensionless	6.67×10^{-5}, 1.75	1	6, 18
Parameter describing scaling of root mass with leaf area	α_3	kg m^{-2}	0.07	1	7, 18
Ratio of bark area to sapwood area	b	dimensionless	0.17		5,18
Production					
Nitrogen mass per leaf area	ν	kg m^{-2}	1.87×10^{-3}	3	12-13
Ratio of light-saturated CO_2 assimilation rate to leaf nitrogen mass	A_0	mol yr^{-1} kg^{-1}	1.78×10^{5}	3	12
Ratio of leaf dark respiration to leaf nitrogen mass	$c_{\mathrm{R,l}}$	mol yr^{-1} kg^{-1}	2.1×10^{4}	3	13
Fine-root respiration per mass	$c_{\mathrm{R,r}}$	mol yr^{-1} kg^{-1}	217	3	13
Sapwood respiration per stem volume	$c_{\mathrm{R,s}}$	mol yr^{-1} m^{-3}	4012	3	13
Yield; ratio of carbon fixed in mass per carbon assimilated	Y	dimensionless (0 to 1)	0.7	3	15
Constant converting assimilated CO_2 to dry mass	c_{bio}	kg mol^{-1}	2.45×10^{-2}	3	15
Parameters describing scaling of turnover rate for leaf with ϕ	α_4,β_4	m^2 kg^{-1} yr^{-1}, dimensionless	2.86×10^{-2}, 1.71	3	14
Turnover rate for bark	k_{b}	yr^{-1}	0.2	2	14
Turnover rate for fine roots	k_{r}	yr^{-1}	1.0	3	14
Seed production					
Accessory costs of seed production	c_{acc}	dimensionless	4.0	3	17
Maximum allocation to reproduction	c_{r1}	dimensionless (0 to 1)	1.0	2	16
Parameter determining rate of change in $r(x,m_l)$ around h_m	c_{r2}	dimensionless	50	2	16
Mortality					
Survival probability during dispersal	π_0	dimensionless (0 to 1)	0.25	2	22
Parameter influencing survival through germination	c_{s0}	kg m^{-2} yr^{-1}	0.1	2	20
Baseline rate for intrinsic mortality	c_{d0}	yr^{-1}	0.52	2,3	21
Risk coefficient for tissue density in intrinsic mortality	c_{d1}	m^3 kg^{-1}	6.5×10^{-3}	3	21
Baseline rate for growth-related mortality	c_{d2}	yr^{-1}	5.5	2,3	21
Risk coefficient for dry-mass production per unit leaf area in growth-related mortality	c_{d3}	yr m^2 kg^{-1}	20.0	2,3	21

Table 3 Range of trait values used in simulations, and resulting vegetation properties. Low, average, and high values for LMA, wood density, and seed size were determined by taking the fifth, fiftieth, and ninety-fifth percentiles from published trait datasets (see "Material and Methods" for details), with *N* indicating the number of species in each dataset. The % change for each trait and vegetation property was calculated as abs(high - low)/average*100.

Trait description	**Symbol**	**Unit**	***N***		**Trait value**	**Average height of leaf area** (m)	**LAI** (dimension less)	**NPP** (kg m^{-2} yr^{-1})	**Biomass density** (kg m^{-2})	**Seed rain** (m^{-2} yr^{-1})
LMA	ϕ	kg m^{-2}	1,700	Low	0.05	7.60	3.19	2.22	4.60	650
				Average	0.11	7.99	3.57	2.25	5.64	946
				High	0.32	7.60	3.72	2.22	6.51	1003
				% change	252	0	15	0	34	37
Wood density	ρ	kg m^{-3}	8,412	Low	345	7.91	3.55	2.25	3.45	1240
				Average	608	7.99	3.57	2.25	5.64	946
				High	969	7.10	3.53	2.26	7.60	536
				% change	103	10	1	0	74	74
Height at maturation	h_m	m^2	n.a.	Low	6	4.94	3.81	2.51	3.78	1924
				Average	12	7.99	3.57	2.25	5.64	946
				High	24	10.08	3.29	1.98	7.12	66
				% change	150	64	14	23	59	196
Seed mass	s	kg	522	Low	2.7×10-7	7.45	3.69	2.32	5.38	121590
				Average	3.8×10-5	7.99	3.57	2.25	5.64	946
				High	1.7×10-3	8.62	3.35	2.13	5.84	23
				% change	4,558	15	9	8	8	12852

FIGURES

Fig. 1 Overview of processes represented in the model. Top, An individual's vital rates are jointly determined by its light environment, size, and traits. The locations where traits influence performance are indicated. Middle, Landscapes consist of a distribution of patches linked by seed dispersal. Disturbances remove all vegetation within a patch. Competitive hierarchies within developing patches are modeled by tracking the height distribution of individuals as patches age after a disturbance. Density corresponds to the number of plants per unit height per unit ground area. The shown density illustrates the predicted size structure for a developing stand with average trait values. Bottom, Vegetation properties were modelled for single-species metapopulations at equilibrium.

Fig. 2 Typical representation of the self-thinning trajectories in a stand with average trait values. At any patch age, the density of individuals (per unit ground area) and average size of individuals (in terms of leaf mass) are calculated by integrating over the size distribution shown in Fig. 1.

Fig. 3 Changes in LAI during the development of a patch with average trait values. The variability in total LAI corresponds to the non-linearity in the thinning phase of Fig. 2 (see main text for details). In addition to total LAI, the LAI of three separate groups of individuals is shown: dominant individuals in first wave of recruitment, subordinate individuals in first wave of recruitment, and all individuals in second wave of recruitment. These three groups correspond to seedlings germinating 1) between 0 and 3.7×10^{-4} yrs; 2) between 3.7×10^{-4} and 11.3 yrs; and 3) after 11.3 yrs.

Fig. 4 Temporal patterns of emergent vegetation properties within single-species stands recovering from disturbance, in a metapopulation with a mean disturbance interval of 30 years. Continuous

lines show patterns for a stand with average trait values. Dotted (dashed) show the corresponding temporal patterns for each trait being altered from its average value to its low (high) value, while keeping the other traits at their average values (Table 3). Inset in top-left plot shows behaviour in the first year after disturbance.

Fig. 5 Dependence of metapopulation averages for LAI and biomass density on trait values, for metapopulations with different mean interval between disturbances and productivity. Bold lines show averages for a metapopulation with mean interval between disturbances of 30 years, corresponding to Fig. 4. Other lines show averages for: a) different disturbance intervals of 15 years (dotted lines), 60 years (short dashed lines), 120 years (long dashed lines); b) different site productivities, resulting from changing the ratio of light-saturated CO2 assimilation rate to leaf nitrogen mass to 90% (dashed lines) and 125% (dotted lines) of its baseline value. See Figs. S7 and S8 for plots of average height, NPP, and equilibrium seed rain.

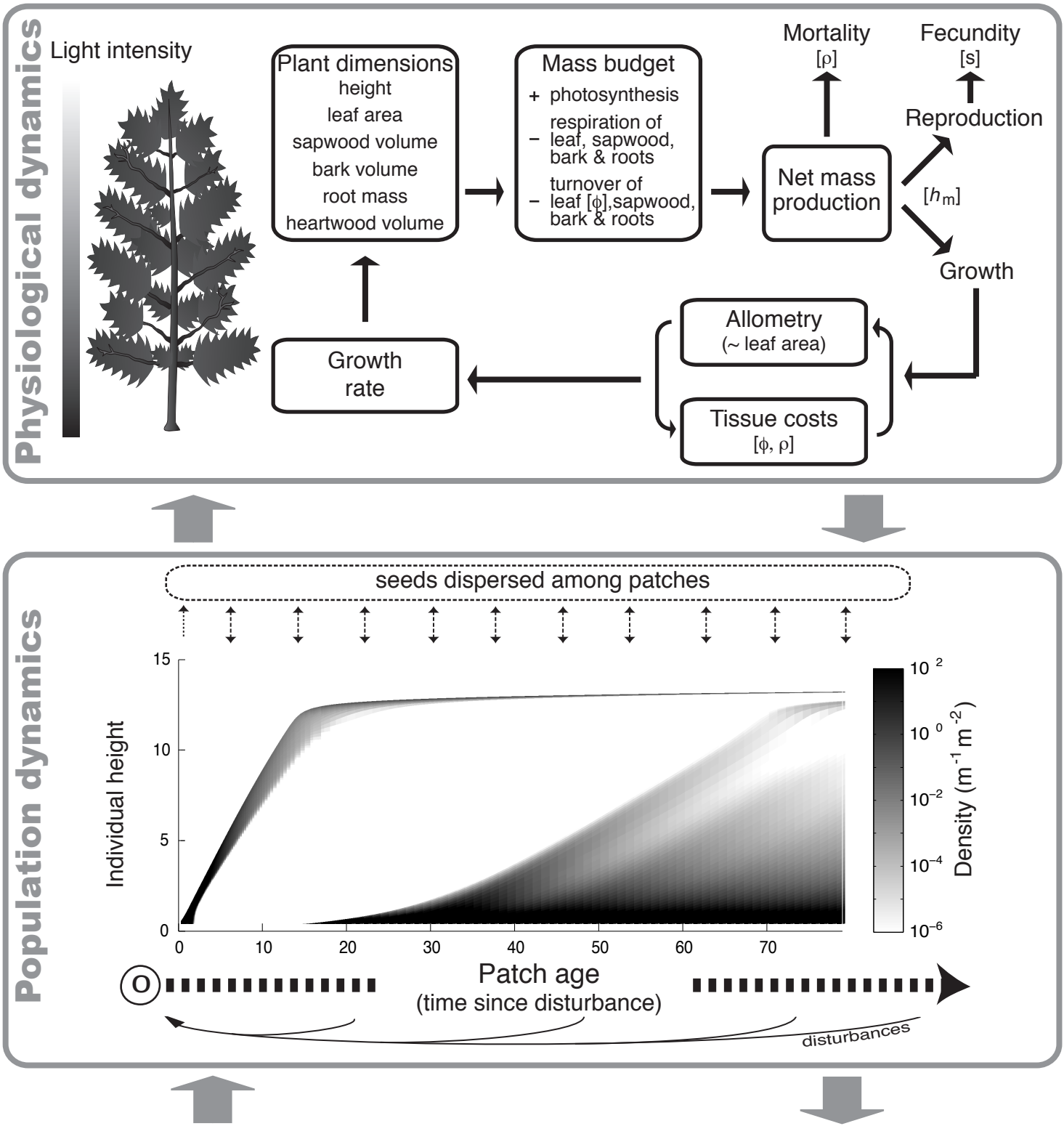
Physiological dynamics
Light intensity
Plant dimensions
height
leaf area
sapwood volume
bark volume
root mass
heartwood volume
Mass budget
+ photosynthesis
− respiration of leaf, sapwood, bark & roots
− turnover of leaf [ϕ],sapwood, bark & roots
Net mass production
Mortality [ρ]
Fecundity [s]
Reproduction
[h_m]
Growth
Allometry (~ leaf area)
Tissue costs [ϕ, ρ]
Growth rate
Population dynamics
seeds dispersed among patches
Individual height
Density (m^{-1} m^{-2})
Patch age
(time since disturbance)
disturbances
Species traits
LMA (ϕ), wood density (ρ), height at maturation (h_m), seed size (*s*)
Vegetation properties
Average height of leaf area (*H*), LAI (*L*), NPP (*N*), biomass density (*B*)

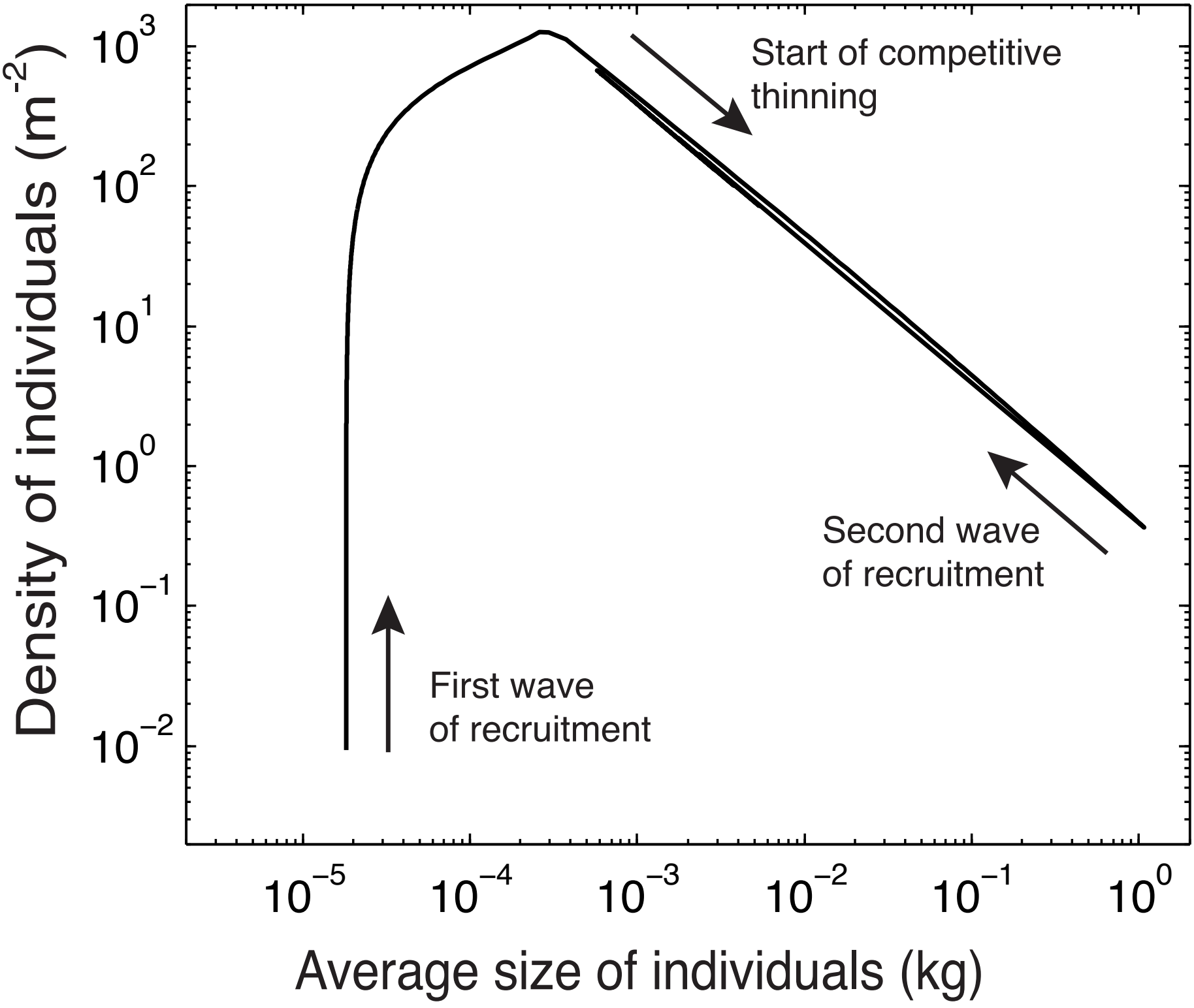
Density of individuals (m^{-2})
10^{3}
10^{2}
10^{1}
10^{0}
10^{-1}
10^{-2}
Start of competitive thinning
Second wave of recruitment
First wave of recruitment
10^{-5}
10^{-4}
10^{-3}
10^{-2}
10^{-1}
10^{0}
Average size of individuals (kg)

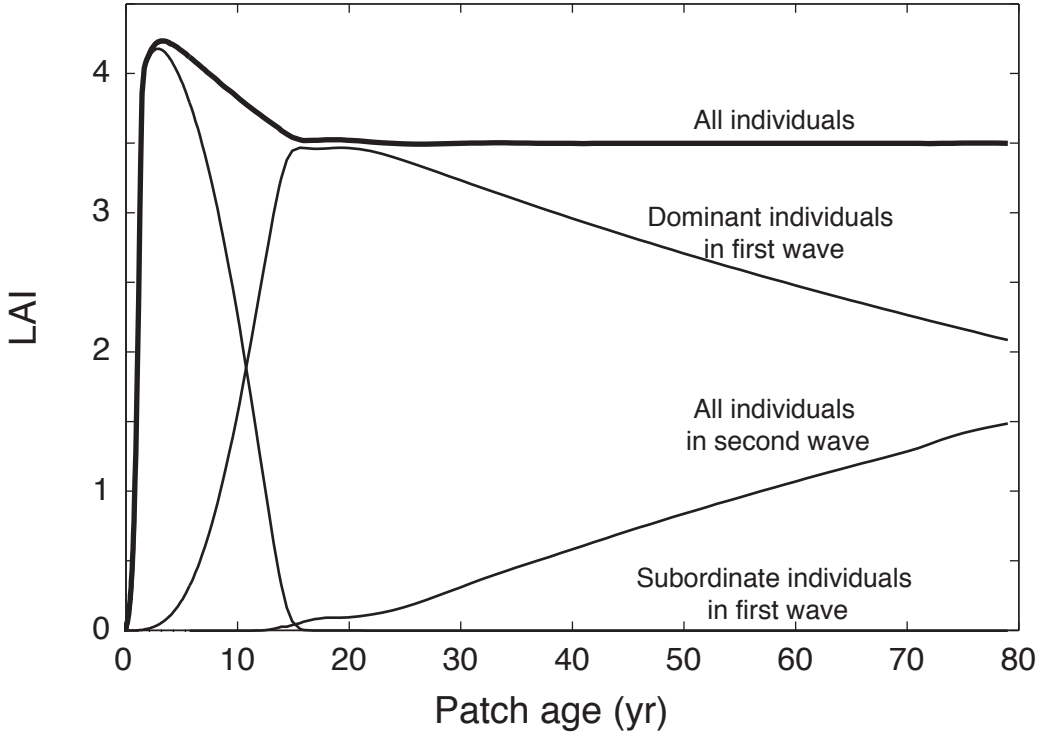
LAI
Patch age (yr)
All individuals
Dominant individuals
in first wave
All individuals
in second wave
Subordinate individuals
in first wave
0
1
2
3
4
0
10
20
30
40
50
60
70
80

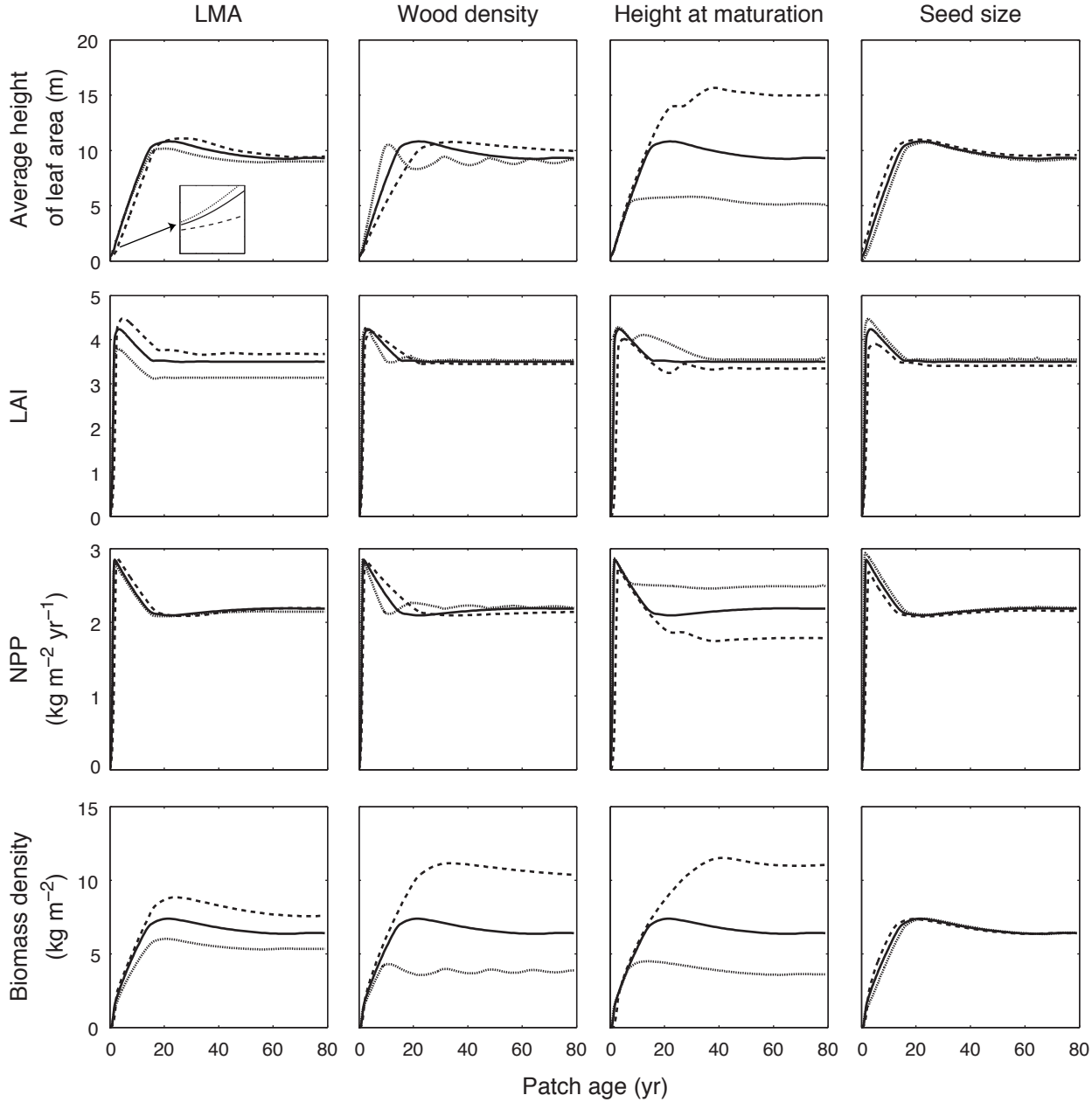
LMA
Wood density
Height at maturation
Seed size
Average height of leaf area (m)
LAI
NPP (kg m^{-2} yr^{-1})
Biomass density (kg m^{-2})
Patch age (yr)

a) Different disturbance intervals

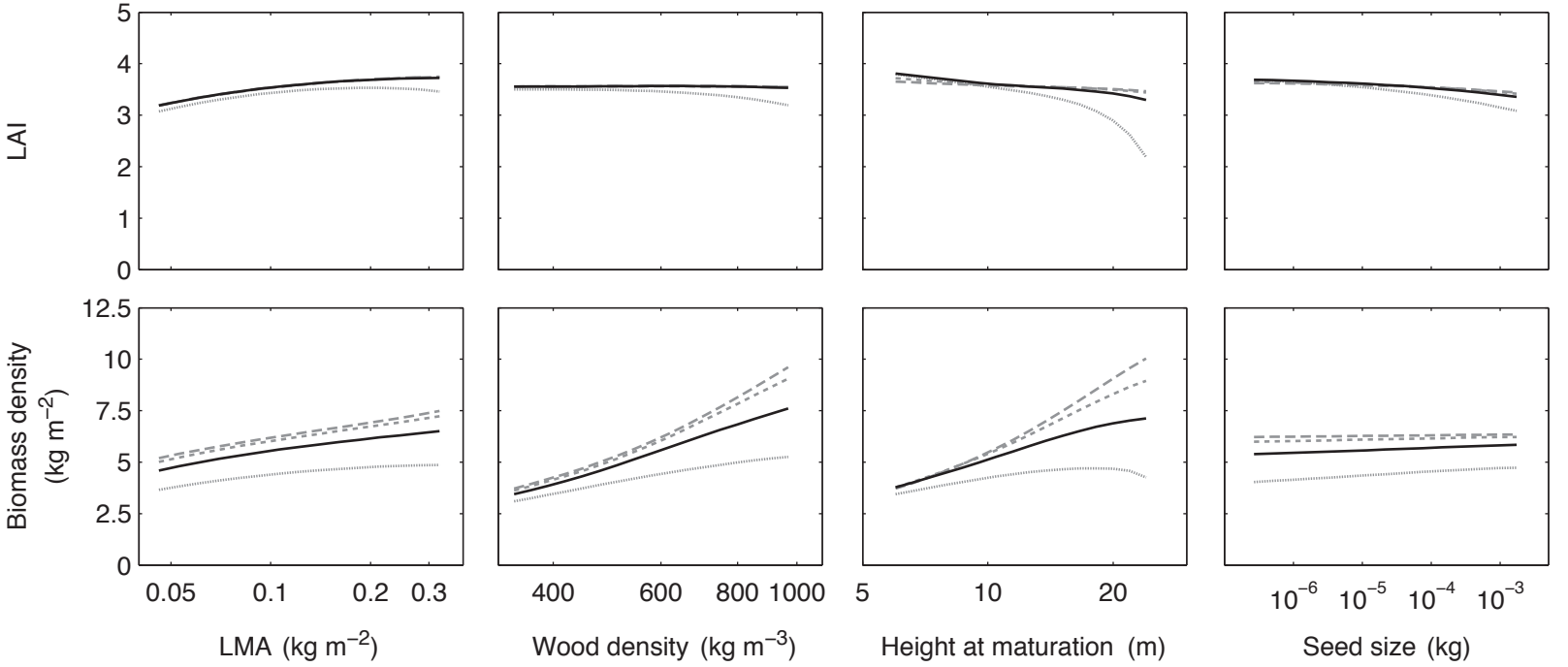

b) Different site productivities

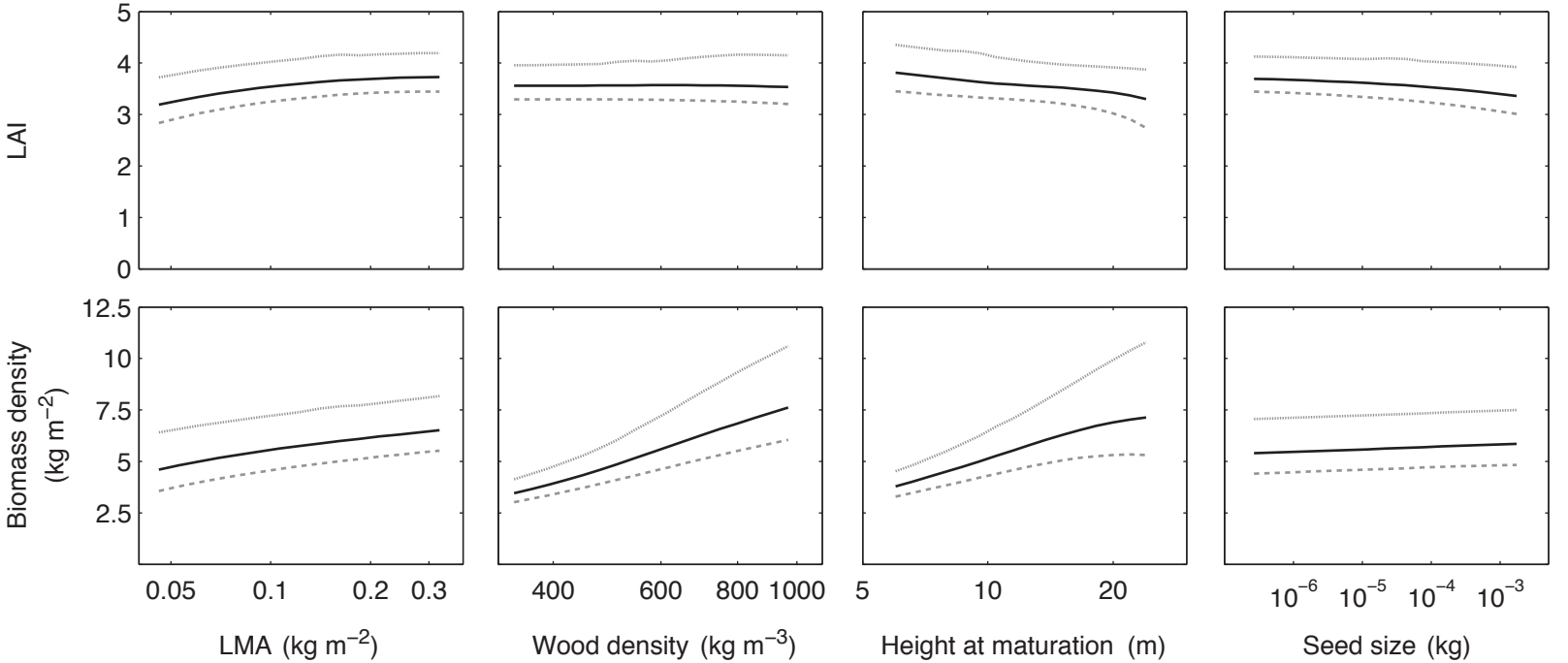

Supporting information

APPENDIX S1 DERIVATION OF EQUILIBRIUM PATCH-AGE DISTRIBUTION

Consider patches of vegetation that are subject to some intermittent disturbance and where the age of a patch corresponds to time since last disturbance. Let $p(a)$ be the frequency density of patches age a at equilibrium and let $\gamma(a)$ be the rate at which patches age a are transformed by disturbance into patches age 0. Then according to the Von Foerster's (1959) equation for age-structured population dynamics, $p(a)$ is given by

$$p(a) = p(0)\Pi(a),$$

where

$$\Pi(a) = \exp\left(\int_0^a -\gamma(\tau)\, \mathrm{d}\tau\right),$$

is the probability that a local population will remain undisturbed for at least a years, and

$$p(0) = \frac{1}{\int_0^\infty \Pi(a)\, \mathrm{d}a},$$

is the frequency density of patches age 0. Assuming the rate of patch disturbance increases linearly with time, e.g. $\gamma(a) = 2\lambda a$, we obtain the following equilibrium distribution:

$$\Pi(a) = e^{-\lambda a^2}, p(0) = 2\left(\frac{\lambda}{\pi}\right)^{0.5}.$$

Noting that the mean disturbance interval $\hat{a} = \frac{1}{p(0)}$, we can express the single unknown parameter, λ, as $\lambda = \frac{\pi}{4\hat{a}^2}$, so $\gamma(a) = \frac{\pi a}{2\hat{a}^2}$. Figure S1 shows the shape of p that results.

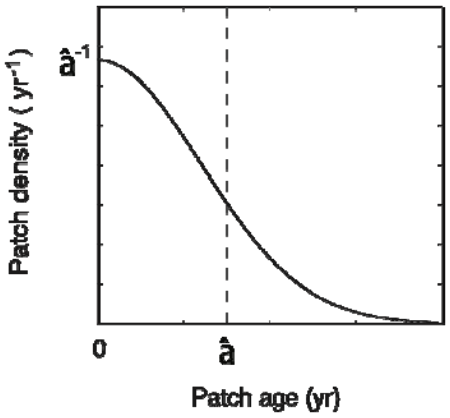

Figure S1 Equilibrium density distribution of patch ages (solid line) in relation mean disturbance interval $\hat{a}$ (dashed line).

APPENDIX S2 DERIVATION OF BIOMASS-ALLOCATION MODEL

Here we derive an allometric model linking the various size dimensions of a plant required by most ecologically realistic vegetation models (i.e. $m_l, m_s, m_b, m_r, m_h, h$ = mass of leaves, mass of sapwood, mass of bark, mass of fine roots, mass of heartwood and plant height respectively) to a single state-dimension: total mass of leaves m_l.

Crown profile and mass of sapwood

We begin with the model of Yokozawa and Hara (1995) describing the vertical distribution of leaf area within the crowns of individual plants. This model can account for a variety of crown profiles through a single parameter η. Setting $\eta = 1$ results in a conical crown, as seen in many conifers, while higher values, e.g. $\eta = 12$, give a top-weighted crown profile similar to those seen among angiosperms. Let $S(z,h)$ be the sapwood area at height z for a plant with top height h, $q(z,h)$ the probability density of leaf area at height z and $Q(z,h)$ be the cumulative fraction of a plant's leaf above height z. Following Yokozawa and Hara (1995) we assume a relationship between $S(z,h)$ and height such that

$$\frac{S(z,h)}{S(0,h)} = \left(1 - \left(\frac{z}{h}\right)^{\eta}\right)^2.$$

We also assume that each unit of sapwood area supports a fixed unit θ of leaf area (pipe model, Shinozaki et al., 1964), so that the total leaf area of a plant relates to basal sapwood area $S(0,h)$:

$$\frac{m_l}{\phi} = \theta S(0,h).$$

The pipe model is assumed to hold within individual plants, as well as across plants of different size. It directly follows that

$$Q(z,h) = \int_z^h q(z',h)\,\mathrm{d}z' = \left(1 - \left(\frac{z}{h}\right)^{\eta}\right)^2.$$

Differentiating with respect to z then yields a solution for the probability density of leaf area as a function of height (Eq. 9). Integrating $S(z,h)$ also gives a solution for the total volume of conductive sapwood in the plant:

$$\frac{m_s}{\rho} = \int_0^h S(z,h)\,\mathrm{d}z = S(0,h)h\eta_c,$$

where $\eta_c = \left(1 - \frac{2}{1+\eta} + \frac{1}{1+2\eta}\right)$ (Yokozawa & Hara 1995). Substituting $S(0,h)$ from above gives an expression for sapwood mass as a function leaf mass (Eq. 4). However, this expression also requires a relation between the plant's height and leaf mass. Based on empirically observed allometries (see below), we assume an allometric log-log scaling relationship between the accumulated leaf area of a plant and its height (Eq. 3).

Bark mass

Bark and phloem tissue are modelled using an analogue of the pipe model, leading to a similar equation (Eq. 5) as that for sapwood mass (Eq. 4). Cross sectional-area of bark per unit leaf area is assumed to be a constant fraction b of the sapwood area per unit leaf area.

Root mass

Consistent with pipe-model assumption, we assume a fixed ratio of root mass per unit leaf area (Eq. 7). Even though nitrogen and water uptake are not modelled explicitly, imposing a fixed ratio of root mass to leaf area ensures that approximate costs of root production are included in calculations of carbon budget.

Heartwood mass

Little is known about longevity of sapwood, or how rates of heartwood production vary with growth rates and traits. Lacking a more mechanistic basis, we take a phenomenological approach to modelling of heartwood mass. Within species, we found that an allometric log-log scaling relationship captured much of the variation between heartwood mass and leaf mass (see Appendix S3). Consistent with the approach taken for sapwood, we assume that the observed relationship between sapwood mass and leaf mass reflects an underlying relationship between the accumulated leaf area and heartwood volume,

$$\frac{m_{\mathrm{h}}}{\rho\eta_{\mathrm{c}}} = \alpha_2\left(\frac{m_{\mathrm{l}}}{\phi}\right)^{\beta_2},$$

where α_2, β_2 are constants and η_{c} adjusts stem volume according to the crown shape, as for sapwood. A corollary of this assumption is that the rate of heartwood production is proportional to rate of leaf mass growth,

$$\frac{\mathrm{d}m_{\mathrm{h}}}{\mathrm{d}t} = \rho\eta_{\mathrm{c}}\phi^{-\beta_2}\alpha_2\beta_2 m_{\mathrm{l}}^{\beta_2-1}\frac{\mathrm{d}m_{\mathrm{l}}}{\mathrm{d}t}.$$

Allocation

Eqs. 2-8 allow all plant dimensions to be calculated from leaf mass. Taking derivatives of these functions gives the change in leaf area, height, sapwood mass, bark mass, heartwood mass, and root mass per unit growth in leaf mass:

$$\frac{\mathrm{d}\omega}{\mathrm{d}m_{\mathrm{l}}}(x, m_{\mathrm{l}}) = \phi^{-1},$$

$$\frac{\mathrm{d}h}{\mathrm{d}m_{\mathrm{l}}}(x, m_{\mathrm{l}}) = \alpha_1\beta_1\omega(x, m_{\mathrm{l}})^{\beta_1-1}\frac{\mathrm{d}\omega}{\mathrm{d}m_{\mathrm{l}}}(x, m_{\mathrm{l}}) = \alpha_1\beta_1\phi^{-\beta_1}m_{\mathrm{l}}^{\beta_1-1},$$

$$\frac{\mathrm{d}m_{\mathrm{s}}}{\mathrm{d}m_{\mathrm{l}}}(x, m_{\mathrm{l}}) = \rho\eta_{\mathrm{c}}\theta^{-1}\left[\frac{\mathrm{d}\omega}{\mathrm{d}m_{\mathrm{l}}}(x, m_{\mathrm{l}})h(x, m_{\mathrm{l}}) + \frac{\mathrm{d}h}{\mathrm{d}m_{\mathrm{l}}}(x, m_{\mathrm{l}})\omega(x, m_{\mathrm{l}})\right] = (1+\beta_1)\rho\eta_{\mathrm{c}}\theta^{-1}\alpha_1\phi^{-1-\beta_1}m_{\mathrm{l}}^{\beta_1},$$

$$\frac{\mathrm{d}m_{\mathrm{b}}}{\mathrm{d}m_{\mathrm{l}}}(x, m_{\mathrm{l}}) = b\frac{\mathrm{d}m_{\mathrm{s}}}{\mathrm{d}m_{\mathrm{l}}},$$

$$\frac{\mathrm{d}m_\mathrm{h}}{\mathrm{d}m_\mathrm{l}} = \rho\eta_\mathrm{c}\alpha_2\beta_2\omega\left(x,m_\mathrm{l}\right)^{\beta_2-1}\frac{\mathrm{d}\omega}{\mathrm{d}m_\mathrm{l}}\left(x,m_\mathrm{l}\right) = \rho\eta_\mathrm{c}\alpha_2\beta_2\phi^{-\beta_2}m_\mathrm{l}^{\beta_2-1},$$

and

$$\frac{\mathrm{d}m_\mathrm{r}}{\mathrm{d}m_\mathrm{l}} = \alpha_3\frac{\mathrm{d}\omega}{\mathrm{d}m_\mathrm{l}}\left(x,m_\mathrm{l}\right) = \alpha_3\phi^{-1}.$$

One way to think of the derivatives $\frac{\mathrm{d}m_\mathrm{s}}{\mathrm{d}m_\mathrm{l}}, \frac{\mathrm{d}m_\mathrm{b}}{\mathrm{d}m_\mathrm{l}}, \frac{\mathrm{d}m_\mathrm{h}}{\mathrm{d}m_\mathrm{l}}$ and $\frac{\mathrm{d}m_\mathrm{r}}{\mathrm{d}m_\mathrm{l}}$ is as the marginal cost of sapwood, bark, heartwood and root needed to support an additional unit of leaf mass. Combining these terms gives the fraction of whole-plant growth that is leaf (Eq. 18), which decreases with increasing size (Figure S6):

$$\begin{aligned}\frac{\mathrm{d}m_\mathrm{l}}{\mathrm{d}m_\mathrm{t}} &= \frac{1}{1+\frac{\mathrm{d}m_\mathrm{s}}{\mathrm{d}m_\mathrm{l}}\left(x,m_\mathrm{l}\right)+\frac{\mathrm{d}m_\mathrm{b}}{\mathrm{d}m_\mathrm{l}}\left(x,m_\mathrm{l}\right)+\frac{\mathrm{d}m_\mathrm{h}}{\mathrm{d}m_\mathrm{l}}\left(x,m_\mathrm{l}\right)+\frac{\mathrm{d}m_\mathrm{r}}{\mathrm{d}m_\mathrm{l}}\left(x,m_\mathrm{l}\right)} \\ &= \frac{1}{1+\left(1+\beta_\mathrm{l}\right)\left(1+b\right)\rho\eta_\mathrm{c}\theta^{-1}\alpha_\mathrm{l}\phi^{-1-\beta_\mathrm{l}}m_\mathrm{l}^{\beta_\mathrm{l}}+\rho\eta_\mathrm{c}\alpha_2\beta_2\phi^{-\beta_2}m_\mathrm{l}^{\beta_2-1}+\alpha_3\phi^{-1}}.\end{aligned}$$

APPENDIX S3 CONFIRMATION OF BIOMASS-ALLOCATION MODEL

We verified the above-ground component of the allometric model using the Coweeta biomass dataset (Martin et al. 1998), which includes mass of aboveground parts (leaf, sapwood, bark, heartwood), other size dimensions (sapwood area at base, stem diameter, plant height) and traits (LMA, WD) for 3-11 individuals from each of 10 species growing in the Southern Appalachian Mountains (USA). After log transforming, most of the different assumptions and predictions from the model can be expressed as bivariate-linear relationships; consequently all tests were performed on log-transformed variables. The strength (r^2) and slope of fitted standardised major-axis lines (Warton et al. 2006) were then used to assess model performance.

The three assumptions of a fixed ratio between leaf area and sapwood area, allometric scaling of height with leaf area, and allometric scaling of heartwood volume with leaf area were all supported by the data (Figure S2). Within species, the slope of fitted allometric relationships between each plant's leaf area and its basal sapwood area did not differ from 1.0 for 9/10 species (Figure S2a), providing good support for the pipe model assumption (across individuals; we were unable to verify whether the pipe model also holds within individuals). Leaf area per sapwood area θ was then estimated by forcing a line of slope 1.0 through the data.

Relationships between height and leaf area (Figure S2b) and heartwood volume and leaf area (Figure S2c) were well approximated by allometric scaling relationships (i.e. with slopes other than 1.0; Table S1).

We tested how well sapwood mass and bark mass could be predicted from leaf area using Eqs. 4 and 5. To do this we calculated average values of θ, ρ, and b for each species (Table S1) and combined these with the species-specific estimates of α_1, β_1 obtained from fitted lines in Figure S2b (Table S1). Thus leaf area, ω, was the only variable differing among individuals within species. Predicted versus observed values for sapwood and heartwood mass were tightly correlated (Figure S3; Table S1), with slopes not significantly different to 1.0 in 17/18 tests, indicating good correspondence between modelled and observed values. The vertical separation among lines fitted to each species in Figure S3a and in Figure S3b could arise from differences in η_c, the single unknown parameter. This parameter adjusts predicted sapwood volume according to crown shape (see Appendix S2). Overall, leaf area accounted for a majority of variance (Table S1) in stem mass and bark mass, lending good support to our approach.

The Coweeta data are almost unique in their coverage; however, we did observe some systematic errors in our model fitting exercise which readers should be aware of. For some individuals (19 of 86), reported volumes for sapwood were greater than reported volumes of all wood. This error is understandable since different methodologies were used to estimate sapwood and total wood volume. The problem arises when estimating heartwood volume, which is given by the difference between total and sapwood volume. To minimise error, we excluded negative estimates of heartwood volume when fitting leaf-area to heartwood-volume relationships (Figure S2c). It is also likely that the Coweeta data overestimates sapwood volume and under estimates heartwood volume, because the heartwood content of branches was not measured. This error can be seen in estimates of η_c obtained from lines fitted to Figure S3a. Values of η_c should be constrained between 0 and 1; however, estimates greater than 1.0 were also obtained, probably because observed values of sapwood mass were too high. While acknowledging these errors, we do not believe they detract from the overall suitability of the Coweeta data for model confirmation and parameterisation.

Figure S2 Observed relationships between (a) leaf area and sapwood area, (b) leaf area and height, and (c) leaf area and heartwood volume in the Coweeta biomass data. Each dot represents a single individual; different symbols and colours indicate different species; coloured lines are standardised major axis line fits (see Table S1 for details). The dotted line shows parameter combinations used in this paper.

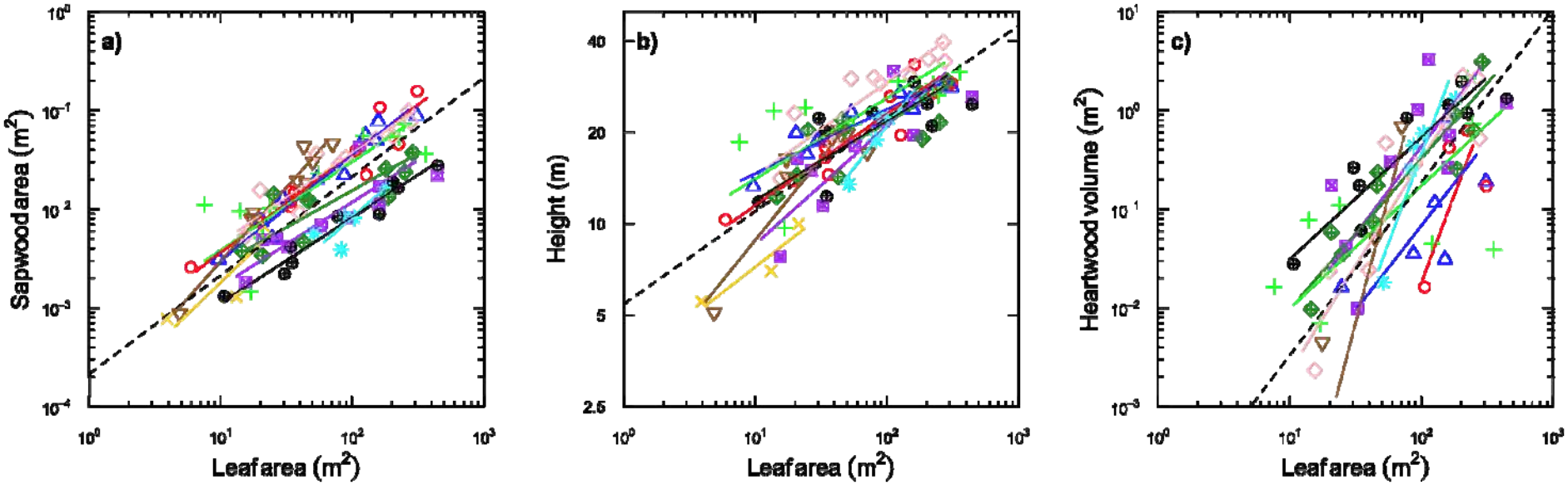

Figure S3 Predicted (x-axis) and observed (y-axis) values for (a) sapwood mass and (b) bark mass in the Coweeta biomass data. Each dot represents a single individual; different symbols and colours indicate different species; coloured lines are standardised major axis line fits; r^2 values given in Table S1. In each plot, there is a single unknown parameter η_c that could potentially explain the vertical separation of lines among species. The dotted line shows a 1:1 relationship based on the value for η_c used in the paper.

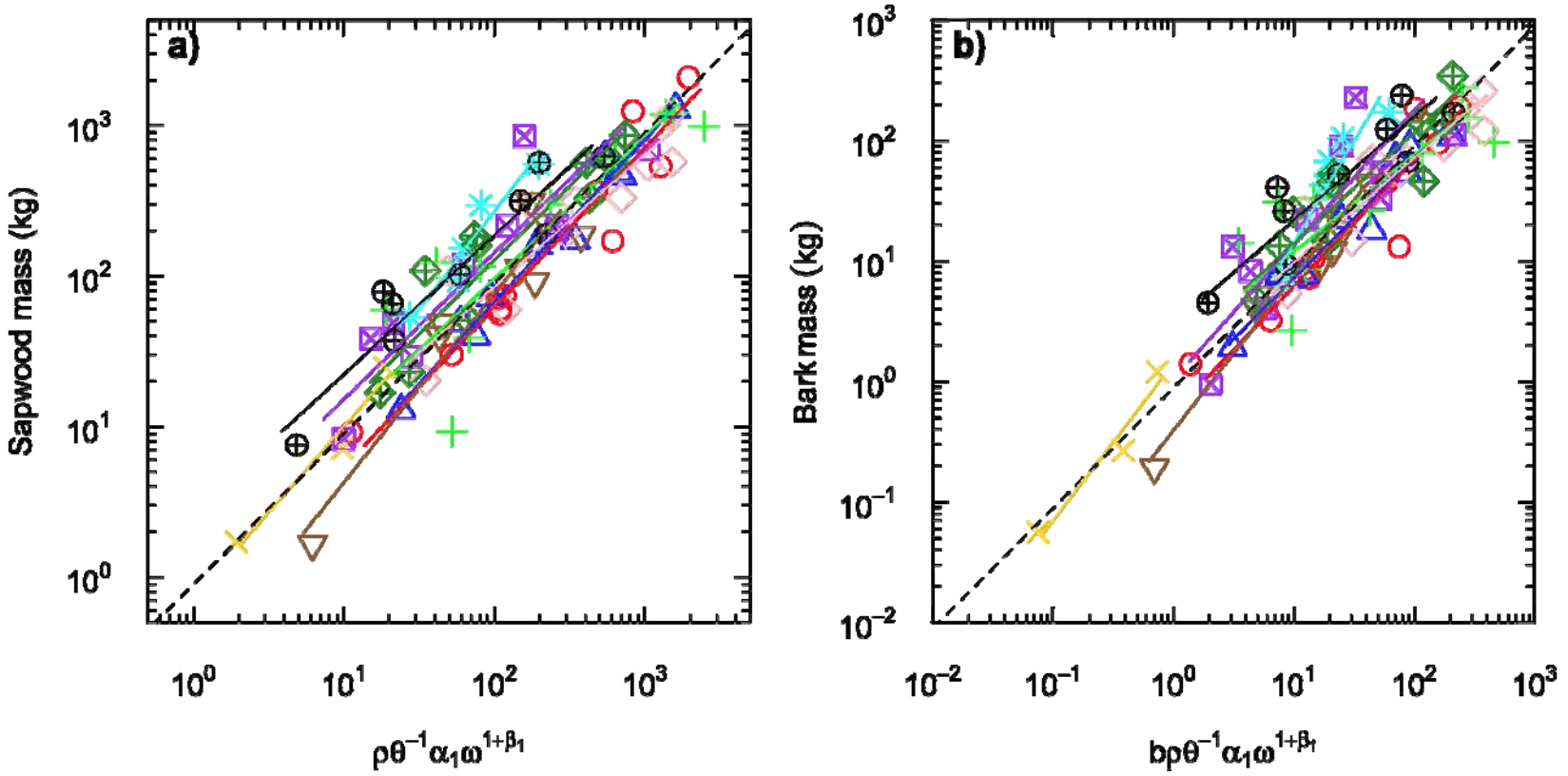

Table S1 Tests of model assumptions and derived trait values for individuals from 10 species contained in the Coweeta biomass dataset. Mean trait values were calculated as geometric means across individuals. Basal sapwood area and leaf area were tightly correlated within species, with all but 1 species having an SMA slope not significantly different from the pipe model assumption of 1.0. Plant height and heartwood volume were each tightly correlated with total leaf area across individuals within each species; derived values of α_1,β_1 and $\eta_c\alpha_2,\beta_2$ were obtained by fitting standardised major-axis lines to observed data. Overall, we found that leaf area explained a large fraction of variance (indicated by r^2 of log-log linear fit) in each of the variables, as assumed by our model. dim = dimensionless.

		Trait values				ASSUMPTION 1: Sapwood area vs. leaf area		ASSUMPTION 2: Height vs. leaf area			ASSUMPTION 3: Heartwood volume versus leaf area			TEST: Relationship to leaf area (r^2)	
Species	n	ϕ (kg m^{-2})	ρ (kg m^{-3})	b (dim)	θ (dim)	r^2	Slope (95% CI) (dim)	r^2	B_1 (dim)	α_1 (m^{-1})	r^2	B_2 (dim)	$\alpha_2\eta_c$ (m)	m_s (kg)	m_b (kg)
Acer rubrum (red maple)	11	0.078	530	0.123	2752	0.90	1.0 (0.79, 1.27)	0.86	0.30	5.74	0.41	3.55	1.44E-9	0.93	0.88
Betula lenta (sweet birch)	10	0.035	505	0.129	2940	0.95	1.07 (0.89, 1.28)	0.86	0.21	9.02	0.44	1.71	2.58E-5	0.97	0.95
Carya ovata (shagbark hickory)	10	0.084	590	0.182	3082	0.64	0.90 (0.56, 1.44)	0.46	0.26	7.64	0.35	1.24	5.65E-4	0.76	0.65
Cornus florida (flowering dogwood)	3	0.036	511	0.039	5449	0.74	1.29 (0.1, 16.93)	0.87	0.34	3.31				0.96	0.95
Liriodendron tulipifera (tulip poplar)	10	0.060	368	0.252	2677	0.86	0.90 (0.66, 1.22)	0.77	0.31	7.06	0.83	2.14	1.66E-5	0.82	0.83
Oxydendrum arboreum (sourwood)	8	0.058	427	0.113	2020	0.95	1.50 (1.19, 1.88)	0.80	0.54	2.57	0.46	5.12	1.48E-10	0.89	0.94
Quercus alba (white oak)	10	0.083	508	0.206	7998	0.70	0.85 (0.55, 1.32)	0.66	0.39	3.49	0.47	1.78	1.17E-4	0.8	0.67
Quercus coccinea (scarlet oak)	5	0.097	451	0.316	12233	0.63	1.18 (0.45, 3.10)	0.85	0.55	1.64	0.84	3.59	2.38E-8	0.92	0.86
Quercus prinus (chestnut oak)	10	0.090	529	0.281	5820	0.70	0.75 (0.49, 1.16)	0.58	0.25	6.71	0.84	1.52	2.91E-4	0.86	0.80
Quercus rubra (red oak)	9	0.086	443	0.398	11765	0.96	0.87 (0.72, 1.05)	0.54	0.26	6.56	0.82	1.23	1.83E-3	0.89	0.80
AVERAGES		**0.068**	**482**	**0.172**	**4669**	**0.80**	**0.977**	**0.73**	**0.306**	**5.44**	**0.61**	**1.75**	**5.91E-5**	**0.88**	**0.83**

APPENDIX S4 RELATIONSHIP BETWEEN MORTALITY AND WOOD DENSITY

We assessed the relationship between wood density and mortality using data compiled from three tropical and one warm temperate site: Pasoh Forest Reserve and Lambir Hills National Park in Malaysia (King et al. 2006), Kuala Belong rainforest in Borneo (Osunkoya et al. 2007) and Yakushima Island in Japan (Aiba & Kohyama 1997). Survival estimates from each study were converted to instantaneous mortality rates assuming a constant mortality per time. Our mortality model (Eq. 21) assumes independent and additive effects of intrinsic and growth-related mortality on overall mortality. Further, we assume a log-linear relationship between intrinsic mortality rate and wood density, which is supported by the data (Figure S4). Even though the size range of individuals sampled differed among the three studies (Aiba: 2-8cm dbh; King: 8-20 cm dbh; Osunkoya: >5cm dbh), a consistent relationship was observed across sites: the fitted lines did not differ significantly in either slope or intercept. Chave et al. (2009) report a similar relationship using data from Barro Colorado Island, Panama.

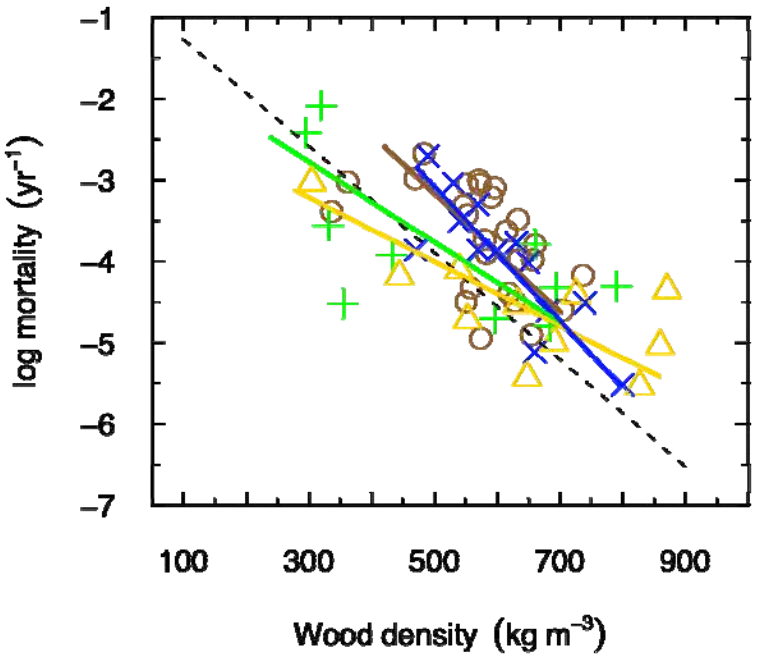

Figure S4 Relationship between wood density and log-transformed mortality rate at four sites. Each dot represents average mortality for a single species; different symbols indicate different sites. The r^2 for relationships within sites ranges from 0.27 - 0.69. The dotted line shows parameter combinations used in this paper.

APPENIX S5 DERIVATION OF SEEDLING GERMINATION-SURVIVAL MODEL

The third line of Eq. 22 gives the boundary condition for the partial differential equation described on line one of Eq. 22. This equation links the density of seedlings at the smallest size in the population (a function of seed mass; Eq. 1) to the prevailing seed rain. For simplicity, we do not model the germination process explicitly. Instead, survival through germination is made contingent on the plants' growth rate, such that only plants with a positive growth rate survive. Seedlings with negative or zero growth are assumed to perish (Eq. 20). Not only is this behaviour biologically desirable, it is also a mathematical necessity, since the boundary condition is only valid when growth rate $g\left(x,m_{\mathrm{l},0},E(\cdot,a)\right)$ is positive. Only seedlings that survive germination are considered to have entered the population and influence shading. Having a larger seed is not considered to have any influence on survival through germination beyond the effect on initial size.

From the boundary condition (third line of Eq. 22), we see that the density of seedlings at the size of germination will decline continuously to zero as growth ceases if the seedling survival through germination $\pi_1\left(x,m_{\mathrm{l},0},E(\cdot,a)\right)$ is chosen so that $\pi_1\left(x,m_{\mathrm{l},0},E(\cdot,a)\right)/g\left(x,m_{\mathrm{l},0},E(\cdot,a)\right)\to 0$ whenever $g\left(x,m_{\mathrm{l},0},E(\cdot,a)\right)\to 0^+$. Note first that by Eq. 19, $g\left(x,m_{\mathrm{l},0},E(\cdot,a)\right)$ = constant × $P\left(x,m_{\mathrm{l},0},E(\cdot,a)\right)$, where the constant depends only on the size $m_{\mathrm{l},0}$ of seedlings. It therefore suffices to consider the behaviour of $\pi_1\left(x,m_{\mathrm{l},0},E(\cdot,a)\right)/P\left(x,m_{\mathrm{l},0},E(\cdot,a)\right)$ as $P\left(x,m_{\mathrm{l},0},E(\cdot,a)\right)\to 0^+$. Ultimately we want seedling survival to be a function of mass production P. Expanding any such function in a Taylor series around $P=0$ gives,

$$\frac{\pi_1(P)}{P}=\frac{\pi_1(0)+\pi_1'(0)P+0.5\pi_1''(0)P^2+O\left(P^3\right)}{P}=\frac{\pi_1(0)}{P}+\pi_1'(0)+0.5\pi_1''(0)P+O\left(P^2\right).$$

Thus, the function for seedling survival must satisfy $\frac{\pi_1(0)}{P}+\pi_1'(0)\to 0$ as $P\to 0^+$, to guarantee that $\pi_1\left(x,m_{\mathrm{l},0},E(\cdot,a)\right)/g\left(x,m_{\mathrm{l},0},E(\cdot,a)\right)$ also approaches zero. The function $\pi_1(P)=\left(\frac{P}{\omega}\right)^2\Big/\left(c_{\mathrm{s}0}{}^2+\left(\frac{P}{\omega}\right)^2\right)$ is one example, which can be rearranged to give Eq. 20. We chose to use dry mass production per leaf area as the primary indicator of survival, to be consistent with the instantaneous mortality function. This function gives a logistic relationship between survival through germination and mass production, declining to zero as $P\to 0^+$.

APPENDIX S6 CALCULATION OF GROSS ANNUAL ASSIMILATION FROM SOLAR PATTERNS

Gross annual CO_2 assimilation for a leaf with maximum photosynthetic capacity $A_0\upsilon$ and at canopy openness $E(z,a)$, i.e. $A_{\mathrm{lf}}(A_0\upsilon, E(z,a))$ from Eq. 12, was calculated by integrating instantaneous rates of assimilation over the diurnal solar cycles experienced at a particular location through the year. Instantaneous rates of CO_2 assimilation were calculated using a rectangular hyperbolae (Figure S5a):

$$A_{\mathrm{inst}}(I, E(z,a), A_0\upsilon) = 0.5\Theta^{-1}\left(\Phi IE(z,a) + A_0\upsilon - \sqrt{(\Phi IE(z,a) + A_0\upsilon)^2 - 4\Theta\Phi IE(z,a)A_0\upsilon}\right),$$

where I is the photon flux above the canopy (mol photons m^{-2} s^{-1}), Φ is the quantum yield of assimilation (= 0.04 mol CO_2 mol $photon^{-1}$ s^{-1}) and Θ is a curvature factor (=0.5) (Cannell & Thornley 1998). Photon flux above the canopy was simulated for each time and day as a function of latitude, date and time using standard solar equations found in software for analysing hemispherical canopy photos (Ter Steege, 1996). Integrating over diurnal variations in solar intensity, we found the relationship between average annual gross assimilation and canopy openness could be perfectly approximated ($r^2 > 0.99$) by the function (Figure S5b):

$$A_{\mathrm{lf}}(A_0\upsilon, E(z,a)) = c_{\mathrm{P1}}\frac{E(z,a)}{E(z,a) + c_{\mathrm{P2}}}.$$

Use of the approximation in simulations gave identical results, but greatly improved computation time. The values for c_{P1} and c_{P2} used in simulations are given in Figure S5.

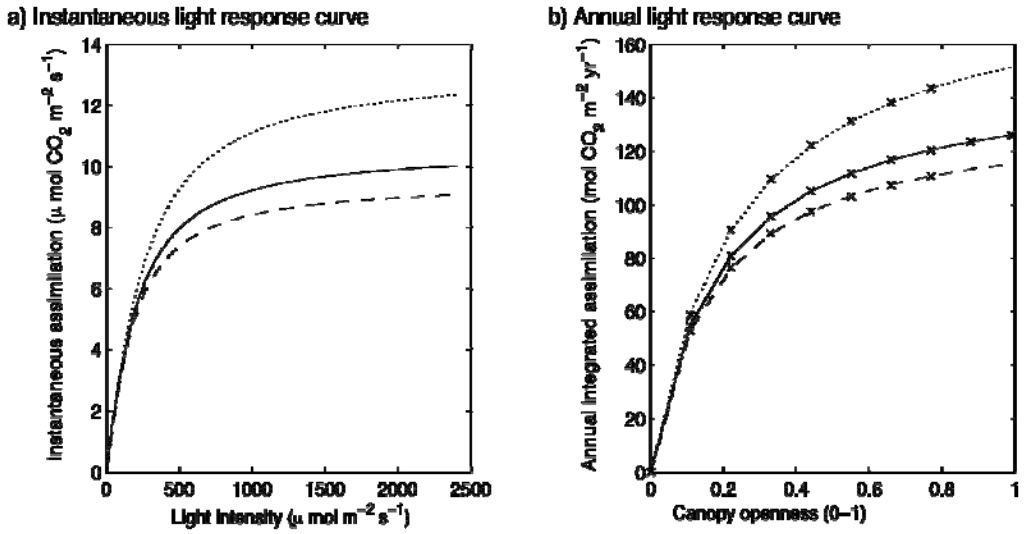

Figure S5 Instantaneous (a) and annual (b) photosynthetic light response curves with nitrogen use efficiency set at 90% (dashed), 100% (solid) and 125% (dotted) of value given in Table 2 of the main text. Annual curves are calculated by integrating the instantaneous curves over the solar regime experienced in Sydney for given levels of canopy openness. Crosses show actual integrated values, lines show approximations based on fitted equations with parameters:
$c_{\mathrm{P1}} = 135.24$, $c_{\mathrm{P2}} = 0.17$ (90%), $c_{\mathrm{P1}} = 150.36$, $c_{\mathrm{P2}} = 0.19$ (100%), and $c_{\mathrm{P1}} = 187.8$, $c_{\mathrm{P2}} = 0.24$ (125%).

APPENDIX S7 MODEL CALIBRATION

PHOTOSYNTHESIS AND RESPIRATION: Global averages for leaf nitrogen content, the ratio of maximum photosynthetic rate to leaf nitrogen content and ratio of dark respiration rate to leaf nitrogen content were calculated using the GLOPNET dataset (Wright et al. 2004), which includes hundreds of site x species measurements. Root respiration (at 20°C) was predicted from nitrogen content using a large data compilation (Reich et al. 2008), assuming nitrogen content for roots of 0.017 kg kg^{-1} (Gordon & Jackson 2000). Sapwood respiration per volume (at 20°C) was estimated as the average of rates from 5 species, measured with extracted wood samples (Spicer & Holbrook 2007). Yield (carbon fixed per carbon assimilated) was set to 0.7 (Thornley & Cannell 2000). Conversion from assimilated CO_2 to kg dry mass is achieved by multiplication with c_{bio} = 2.45E-2, given by 0.49 x 12E-3 kg C mol^{-1} CO_2, where 0.49 is the carbon fraction of biomass (Roderick et al. 1999).

TURNOVER: LMA was related to leaf turnover rate (1/ leaf lifespan) based on observed in the GLOPNET dataset (Wright et al. 2004). Turnover rate of bark was assumed to be 0.2, while turnover rate of fine roots was assumed to be 1.0 following (Jackson, Mooney, & Schulze 1997).

BIOMASS ALLOCATION: In verifying the biomass allocation model with the Coweeta dataset, we detected species differences in θ, b, and in the intercepts of scaling relationships between height and total leaf area, and heartwood volume and total leaf area. The slopes of these scaling relationships did not differ significantly among species (p=0.055, p=0.07), though intercepts did. We therefore used the estimated common slope together with the average intercept, calculated by forcing a line with common slope through the data for each species and averaging the intercept term across species. θ and b were set to the geometric mean across species, given in Table S1. We assumed a crown shape parameter of 12, which equates to a crown with 98.4% of its leaf area in the top third of each plant, and a value of $\eta_c = 0.886$. Combining this with the estimated vale of $\alpha_2 \eta_c = 5.91\mathrm{E}-5$ gives the value of α_2 shown in Table 2. The ratio of root mass to leaf area was determined using data for saplings of 18 tropical species (Aiba & Nakashizuka 2005), with an average value of 0.07 across species.

FECUNDITY: Based on data for 14 species, average accessory costs of reproduction were estimated to be 3 times the weight of seed produced (Lord & Westoby 2006)

MORTALITY: The risk coefficient (c_{d1}) for wood density in Eq. 21 was set to value of the common slope line fitted to empirical data in Figure S4. We then set the baseline rate (c_{d0}) for intrinsic mortality so that an individual with global average wood density (608 kg m^{-3}, as per Table 3 main text) would have an intrinsic mortality of 0.01 yr^{-1}. The value of 0.01 was selected as a value at the lower end of observed rates (Muller-Landau et al. 2006; Coomes & Allen 2007). We adopted a baseline rate lower than the observed rate in Figure S4 because observed data include both intrinsic and growth-related mortality. The baseline mortality for growth-related mortality (c_{d2}) was chosen so that growth-related mortality for a plant with carbon balance of zero was 5.5. The coefficient of carbon income in Eq. 21 (c_{d3}) was set to 20 so as to give a sharp increase in mortality as carbon income approaches zero. Survival through dispersal was assumed to be 25%. The single constant determining survival through germination (c_{s0}) was set at 0.1 kg m^{-2} yr^{-1}, approximately 10% of the mass production rate of a seedling with global average traits growing in full light (1.018 kg $m^{-2}yr^{-1}$).

COMPETITIVE INTERACTIONS: White et al. (2000) suggest a value of 0.5 for the extinction coefficient of light as suitable for most canopy types.

REFERENCES

Aiba, M. & Nakashizuka, T. (2005) Sapling structure and regeneration strategy in 18 Shorea species co-occurring in a tropical rainforest. *Annals of Botany*, **96**, 313-321.

Aiba, S. & Kohyama, T. (1997) Crown architecture and life-history traits of 14 tree species in a warm- temperate rain forest: significance of spatial heterogeneity. *Journal of Ecology*, **85**, 611-624.

Cannell, M.G.R. & Thornley, J.H.M. (1998) Temperature and CO[2] responses of leaf and canopy photosynthesis: a clarification using the non-rectangular hyperbola model of photosynthesis. *Annals of Botany*, **82**, 883-892.

Chave, J., Coomes, D.A., Jansen,, S., Lewis, S.L., Swenson, N.G. & Zanne, A. (2009) Towards a worldwide wood economics spectrum. *Ecology Letters*, **12**, 351-366.

Coomes, D.A. & Allen, R.B. (2007) Mortality and tree-size distributions in natural mixed-age forests. *Journal of Ecology*, **95**, 27-40.

Gordon, W.S. & Jackson, R.B. (2000) Nutrient concentrations in fine roots. *Ecology*, **81**, 275-280.

Jackson, R.B., Mooney, H.A. & Schulze, E. (1997) A global budget for fine root biomass, surface area, and nutrient contents. *Proceedings of the National Academy of Science, USA*, **94**, 7362-7366.

King, D.A., Davies, S.J., Tan, S. & Noor, N.S.M. (2006) The role of wood density and stem support costs in the growth and mortality of tropical trees. *Journal of Ecology*, **94**, 670-680.

Lord, J.M. & Westoby, M. (2006) Accessory costs of seed production. *Oecologia*, **150**, 310-317.

Martin, J.G., Kloeppel, B.D., Schaefer, T.L., Kimbler, D.L. & McNulty, S.G. (1998) Aboveground biomass and nitrogen allocation of ten deciduous southern Appalachian tree species. *Canadian Journal of Forest Research*, **28**, 1648-1658.

Muller-Landau, H.C., Condit, R.S., Chave, J., Thomas, S.C., Bohlman, S.A., Bunyavejchewin, S., Davies, S.J., Foster, R., Gunatilleke, S., Gunatilleke, N., Harms, K.E., Hart, T., Hubbell, S.P., Itoh, A., Kassim, A., Lafrankie, J.V., Lee, H.S., Losos, E., Makana, J., Ohkubo, T., Sukumar, R., Sun, I., Nur Supardi, M.N., Tan, S., Thompson, J., Valencia, R., Munoz, G.V., Wills, C., Yamakura, T., Chuyong, G., Dattaraja, H.S., Esufali, S., Hall, P., Hernandez, C., Kenfack, D. & Kiratiprayoon, S. (2006) Testing metabolic ecology theory for allometric scaling of tree size, growth and mortality in tropical forests. *Ecology Letters*, **9**, 575-588.

Osunkoya, O.O., Sheng, T.K., Mahmud, N. & Damit, N. (2007) Variation in wood density, wood water content, stem growth and mortality among twenty-seven tree species in a tropical rainforest on Borneo Island. *Austral Ecology*, **32**, 191-201.

Reich, P.B., Tjoelker, M.G., Pregitzer, K.S., Wright, I.J., Oleksyn, J. & Machado, J. (2008) Scaling of respiration to nitrogen in leaves, stems and roots of higher land plants. *Ecology Letters*, **11**, 793-801.

Roderick, M.L., Berry, S.L., Saunders, A.R. & Noble, I.R. (1999) On the relationship between the composition, morphology and function of leaves. *Functional Ecology*, **13**, 696-710.

Shinozaki, K., Yoda, K., Hozumi, K. & Kira, T. (1964) A quantitative analysis of plant form - the pipe model theory. I. Basic analyses. *Japanese Journal of Ecology*, **14**, 97-105.

Spicer, R. & Holbrook, N.M. (2007) Effects of carbon dioxide and oxygen on sapwood respiration in five temperate tree species. *Journal of Experimental Botany*, **58,** 1313-1320.

Ter Steege, H. *Winphot 5: a programme to analyze vegetation indices, light and light quality from hemispherical photographs. 1996. Tropenbos Guyana Reports. Georgetown, Guyana: Tropenbos Guyana Programme*.

Thornley, J.H.M. & Cannell, M.G.R. (2000) Modelling the components of plant respiration: representation and realism. *Annals of Botany*, **85**, 55-67.

Von Foerster, H. (1959) Some remarks on changing populations. *The kinetics of cellular proliferation (F. Stohlman eds.)*. pp. 382-407. Grune et Stratton, New York.

Warton, D.I., Wright, I.J., Falster, D.S. & Westoby, M. (2006) Bivariate line-fitting methods for allometry. *Biological Reviews*, **81**, 259-291.

White, M.A., Thornton, P.E., Running, S.W. & Nemani, R.R. (2000) Parameterization and sensitivity analysis of the BIOME–BGC terrestrial ecosystem model: net primary production controls. *Earth Interactions*, **4**, 1-85.

Wright, I.J., Reich, P.B., Westoby, M., Ackerly, D., Baruch, Z., Bongers, F., Cavender-Bares, J., Chapin, F., Cornelissen, J., Diemer, M., Flexas, J., Garnier, E., Groom, P., Gulias, J., Hikosaka, K., Lamont, B., Lee, T., Lee, W., Lusk, C., Midgley, J., Navas, M., Niinemets, Ü., Oleksyn, J., Osada, N., Poorter, H., Poot, P., Prior, L., Pyankov, V., Roumet, C., Thomas, S., Tjoelker, M., Veneklaas, E. & Villar, R. (2004) The world-wide leaf economics spectrum. *Nature*, **428**, 821-827.

Yokozawa, M. & Hara, T. (1995) Foliage profile, size structure and stem diameter plant height relationship in crowded plant-populations. *Annals of Botany*, **76**, 271-285.

Figure S6 The influence of plant size on allocation and dry mass production. (a) With increasing size, a larger fraction of an individual's mass is allocated to support tissues, in the form of bark, sapwood and heartwood. (b) Dry mass production is determined by the difference between an individuals' photosynthetic income (dotted lines, each line showing total income at a different level of canopy openness, E) and the sum of respiration and turnover costs (solid and dashed lines). Total support costs increase with height, which leads to an increase in minimum light requirement with size (solid circles). Income and costs are shown per leaf area. These plots were created using the parameters and global average trait values given in Tables 2 and 3 in the main text.

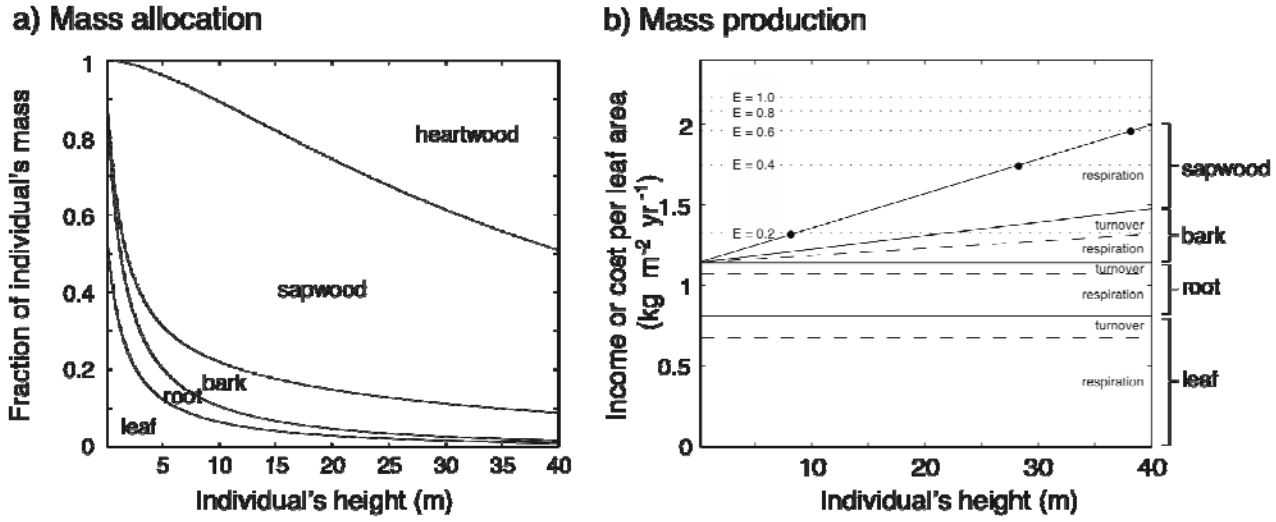

Figure S7 Dependence of emergent properties of vegetation and equilibrium seed rain on trait values, for metapopulations with different mean interval between disturbances. Bold lines show averages for a stand with mean interval between disturbances of 30 years, corresponding to Fig. 4 in the main text. Other lines show corresponding averages for different disturbance intervals of 15 years (dotted lines), 60 years (short dashed lines), 120 years (long dashed lines).

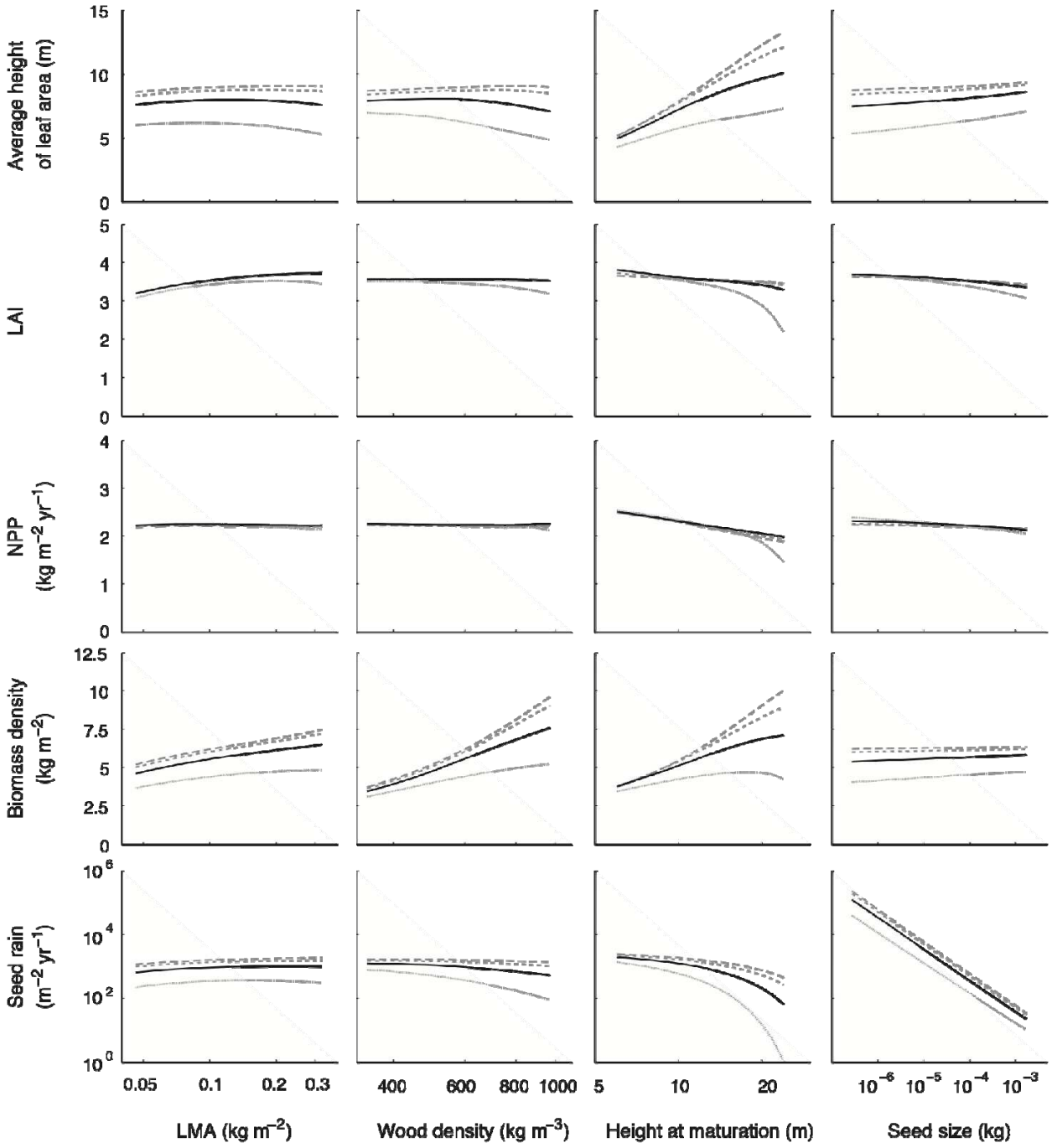

Figure S8 Dependence of emergent properties of vegetation and equilibrium seed rain on trait values, for metapopulations with different productivity. Bold lines show averages corresponding to Fig. 4 in the main text. Other lines show corresponding averages for different site productivities, resulting from changing the ratio of light-saturated CO2 assimilation rate to leaf nitrogen mass to 90% (dashed lines) and 125% (dotted lines) of its baseline value (Table 2 in main text).